Expression of C184M in Primary Cardiac Myofibroblasts and Its Role in Contractility and Collagen Production in NIH 3T3 Fibroblasts

By

Mansoreh Nazari

A Thesis submitted to the Faculty of Graduate Studies of
The University of Manitoba
in partial fulfilment of the requirements of the degree of

MASTER OF SCIENCE

Department of Physiology
University of Manitoba
Winnipeg

ABSTRACT

Cardiovascular disease is the leading cause of morbidity and mortality in adult Canadian men and women and accounts for the greatest financial burden on the health care system across Canada. Coronary artery disease and associated myocardial infarction remain very common forms of heart diseases. Myocardial infarction (MI) induces an initial inflammatory response by formation of granulation tissue and reparative fibrosis. Transforming growth factor β1 (TGF-β1) is a crucial mediator in cardiac repair and remodeling. It plays an important role in suppression of inflammation, phenotypic conversion of fibroblasts to myofibroblasts and deposition of extracellular proteins including collagen types I and III. Myofibroblasts are activated fibroblasts which are hypersynthetic for extracellular matrix; they are contractile cells.

Release of TGF-β1 in the infarct zone also implies activation of a subcellular signal, involving downstream mediators such as receptor regulated Smads (R-Smads) and co-mediator Smads (Co-Smads). TGF-β1 signaling is controlled through endogenous inhibitors, including I-Smad7 and c-Ski.

The current study addresses the expression of C184M, a novel c-Ski binding partner, in cardiac myofibroblasts and the role of this protein in the regulation of myofibroblast contractility and collagen deposition in mouse embryonic fibroblast cells (NIH 3T3 cell line). C184M is a 189 amino acid protein which binds c-Ski and inhibits TGF-β1 signaling pathway by sequestering R-Smads in the cytosol. It is a cytosolic protein which associates with c-Ski via a leucine-rich region. As TGF-β1 plays a central role in the genesis of cardiac fibrosis and scar maturation following myocardial infarction, and it is understood that C184M is a likely player in TGF-β1 signaling, we

rationalized that C184M may play a pivotal role in regulating myofibroblasts function. Herein we characterize the expression of C184M in cardiac myofibroblasts and NIH 3T3 cells using reverse transcription polymerase chain reaction (RT-PCR) and Western blotting. We examined the effect of TGF-β1 on the localization of C184M protein and observed the localization of Smad3 in C184M overexpressing myofibroblasts. These studies were conducted using immunofluorescence staining of cells. We studied the putative interaction between C184M and Smad3 using co-immunoprecipitation, and explored the role of C184M on contractility and collagen secretion in NIH 3T3 cells using collagen gel deformation assays and pro-collagen-1 N-terminal Peptide (P1NP) secretion as a measure of mature collagen production, respectively.

We found that C184M is expressed in primary cardiac fibroblasts isolated from rat heart (P0), and first (P1) and second passage (P2) cardiac myofibroblasts, and NIH 3T3 fibroblasts. Thus, in this instance, NIH 3T3 fibroblasts are a suitable model for primary fibroblasts, in the context of C184M function. Western blot analysis revealed that the C184M is not responsive to TGF-β1 treatment (10ng/ml, 12, 24 and 48hr treatments). In the presence of overexpressed C184M, immunofluorescence studies indicated a shift in localization of Smad3 from a diffuse cytosolic pattern to a distinctly punctate cytosolic pattern, whereas no changes in localization of C184M was found following TGF-β1 treatment (10ng/ml, 24 hr treatment). Analysis of procollagen type I amino terminal (P1NP) secretion in C184M overexpressing NIH 3T3 fibroblasts revealed an increase in P1NP secretion compared to controls. However, C184M overexpression in the presence of TGF-β1 treatment (10ng/ml, 24h), caused a reduction in collagen secretion compared to TGF-β1 stimulation alone. Finally 2D floating gel deformation assays revealed that

C184M overexpression resulted in a significant decrease in contractility of TGF-β1 stimulated (10ng/ml, 24hr treatment) cells.

Our results demonstrate that C184M overexpression abrogates the effects of TGF-β1-mediated increased collagen synthesis in NIH 3T3 fibroblasts. Further, C184M is involved in modulation of contractility of NIH 3T3 fibroblasts. These results support the hypothesis that C184M plays a major role in regulating cardiac myofibroblasts function via its action on the subcellular TGF-β1 signaling pathway.

Acknowledgments

First and foremost I offer my sincerest gratitude to my supervisor, Dr Ian M. C. Dixon, who has supported me throughout my thesis with his patience and knowledge whilst allowing me the room to work in my own way. Without him this thesis would not have been completed or written. One simply could not wish for a better or friendlier supervisor. I gratefully acknowledge my committee members Dr. Mary Lynn Duckworth, Dr Robert Shiu and specially Dr. Nasrin Mesaeli for their advice and crucial contribution, which triggered and nourished my intellectual maturity that I will benefit from, for a long time to come.

I would like to express my gratitude to the head of the department of Physiology, Dr. Janice Dodd, and Ms. Gail McIndless and Judith Olfert and Dr. Peter Zahradka for their support during my transition period and speeding up the procedure for transferring me to Dr. Dixon's lab.

I am much indebted to Ryan Cunnington for his valuable advice in science discussion and tutoring me in the more methods necessary to complete my thesis and how to analyze the data. I also benefited by outstanding works from Krista Bath with her particular skill in molecular techniques. Many thanks go to Sunil Rattan for pleasure working together, as well as keeping me stocked with general supplies. I was blessed to work with Steve Jones and Kristen Bedosky in a pleasant lab atmosphere early in my practical benchtop work. I gratefully thank Dr. Michael Czubryt, for giving me the opportunity to work on his qPCR equipment in his lab. Thanks also to Josette Douville, for her qPCR technical assistances and her scientific advice that made my experiment

fruitful as early as possible – and also to Bernard Abernicia, Leon Espira, Angela Ramjiawan and Dr. Kardami's fellows, who were always ready to lend a hand.

My special thanks go to Dr. Mark Hnatowich, Dr. Hamid Mesaeli, Dr. Barbara Nickle for their invaluable advice and willingness to share their bright thoughts to troubleshoot my RT-PCR and co-immunoprecipitation experiments. I am proud to recognize the support of the Institute of Cardiovascular Sciences that was required to produce and complete my thesis and the MHRC has funded my studies.

Finally, I am extraordinarily fortunate for having a wonderful family. My mother deserves special mention for her inseparable support, prayers and showing me the joy of intellectual pursuit ever since I was a child. My elder sister, Leila, whose, caring is unforgettable and I could never experience education in Canada without her support. Roya, Alireza and Mohammadreza thanks for being caring siblings. Words fail me to express my appreciation to my husband, Hassan Zareh, whose patience and love has taken the load off my shoulder during this experience. His exceptional dedication was extraordinary and admirable. I would like to thank everybody who was important in successful realization of this thesis.

To my family

TABLE OF CONTENTS

List of Figures

List of Abbreviation

α-SMA	α-smooth muscle actin
BCA	bicinchoninic acid
BMDC	bone marrow derived cells
BMP	bone morphogenetic protein
BSA	bovine serum albumin
CAD	coronary artery disease
CBP	CREB-binding protein
Co-Smad	Co-mediator Smads
DDW	double deionized water
DPC4	deleted in pancreatic carcinoma, locus 4
DMEM	Dulbecco's Modified Eagle Medium
DTT	dithiothreitol
ECM	extra cellular matrix
ER	endoplasmic reticulum
FACS	fluorescence activated cell Sorting
GDF	growth and differentiation factor
HEK 293	human embryonic kidney 293 cells
HIPK2	homeodomain-interacting protein kinase 2
I-Smad	inhibitory Smad
MAD	mother against decapentaplegic
MH1	Mad homology 1
MH2	Mad Homology 2
MI	myocardial infarction
MMP	matrix metalloproteinases
N-CoR	nuclear hormone receptor Co-repressor
NIH 3T3	mouse embryonic fibroblast cell line
ORF	open reading frame
P0	passage 0

P1	passage 1
P2	passage 2
PBS	phosphate buffered saline
PFA	paraformaldehyde
qPCR	quantitative polymerase chain reaction
R-Smad	receptor-regulated Smad
RT-PCR	reverse transcriptation polymerase chain reaction
SARA	Smad anchoring protein for receptor activation
SDS	sodium dodecyl sulfate
SMEM	minimum essential medium
Smemb	embryonic isoform of smooth muscle myosin
TβRI	TGF-β type I receptor
TβRII	TGF-β type II receptors
TBS	Tris-buffered Saline
TBS-T	Tris-buffered Saline with 0.2% Tween 20
TGF-β	transforming growth factor-β
TIMP	tissue inhibitor of matrix metalloproteinase

I. Introduction

Cardiovascular diseases are the leading cause of death in virtually all developed countries. Major classes of cardiovascular disease include coronary artery disease, cerebrovascular disease, hypertension, peripheral artery disease, rheumatic heart disease, congenital heart disease and heart failure. Coronary artery disease (CAD) is mainly caused by high concentrations of low-density lipoprotein cholesterol, and subsequent atherosclerosis. Narrowed blood vessels are more susceptible to occlusion due to blood clots. Blockage of coronary arteries results in an inadequate blood supply to the myocardium and resulting in ischemia and myocardial infarction (MI) [1, 2].

Infarction of the myocardium triggers an inflammatory cascade that ultimately results in wound healing and formation of a scar. Infarct healing causes structural changes in the left ventricle, termed "ventricular remodeling", a complex process which ultimately results in dilatation, hypertrophy, and enhanced sphericalization of the ventricle. These geometrical and architectural changes in ventricle structure impair ventricular function and finally lead to heart failure [3, 4].

Myofibroblasts are phenotypically modified fibroblasts, that express relatively high amounts of α-smooth muscle actin (α-SMA) [5-7]. Myofibroblasts are able to contract and exert tensile force on the surrounding ECM and thus provide an effective means to impart scar shrinkage [8]. Myofibroblasts account for the major source of fibrillar collagens in the atria and ventricle after MI [9, 10]. Deposition of fibrillar collagen type I and III in the damaged area strengthens the damaged tissue and prevents ventricular rupture due to mechanical weakening that occurs in the necrotic and inflamed myocardium [11]. Although

secretion of collagen in the infarcted area is beneficial and contributes to wound healing, chronically activated repair mechanisms may result in excessive production of fibrillar collagens, causing increased stiffness marked by diastolic and systolic dysfunction [12].

Transforming growth factor β (TGF-β) is a pleiotropic cytokine, which is markedly expressed in the infarcted myocardium and plays central roles in inflammatory and fibrotic phases of wound healing [13-16]. In addition to nonspecific mechanical force input, bioactive TGF-β modulates the phenotypic switching of fibroblasts to myofibroblasts, and promotes fibrosis [17-19]. The TGF-β signal is transduced from membrane to nucleus through Smad-dependent pathways and regulates ECM protein gene expression [20]. Ski is a nuclear oncoprotein and a TGF-β repressor which can be recruited in TGF-β responsive promoters through association with Smad2, Smad3 and Smad4 proteins [21-24] , where it plays an inhibitory role in the expression of TGF-β responsive genes [25, 26]. The expression of Ski is enhanced during wound healing [27]. Ski negatively regulates TGF-β signaling pathway through disruption of the active heteromeric complex formed between Co-Smad and R-Smads [28]. In addition Ski may interact with other co-repressors, to recruit histone deacetylase complex to the target TGF-β responsive promoters and represse transcription of the corresponding genes [29-30]. Ski also competes with transcriptional co-activator of Smads, and recruits histone deacetylase complex to the target genes to repress transcription [31 32]. Furthermore, the association of Ski with its novel binding partner C184M, is known to inhibit the nuclear translocation of Smad2 in CV-1 cells (monkey kidney cell line)[33].

C184M is a cytosolic protein with 189 amino acids, which interacts with C-terminal coiled-coil region of Ski through its leucine-rich motif, and sequesters Ski in the

cytosol. Consistent with this, Ski is accumulated in the cytosol of hepatocytes which express high level of C184M. In addition C184M suppresses the activity of promoters containing the Smad-binding sites and prevents TGF-β-induced growth inhibition of mink lung Mv1Lu cells [34]. Nonetheless, the role of C184M in TGF-β mediated cell functions that results in fibrosis is unclear. The current series of studies were conducted to investigate the expression of C184M in myofibroblasts and NIH 3T3 fibroblasts and to explore the localization of C184M in myofibroblasts. We also investigated the localization of Smad3 in overexpressing C184M myofibroblasts and examined the effect of C184M overexpression on contractility and collagen secretion in fibroblasts. In the current study, we have documented the expression of C184M in ventricular fibroblasts, myofibroblasts and NIH 3T3 fibroblasts. We also observed that C184M is localized in the cytosol of myofibroblasts and that it accumulates proximal to the nucleus. We showed that Smad3 distribution in cardiac myofibroblasts is altered in association with C184M overexpression. We also confirmed that overexpression of C184M alone (with no other stimulus) induces collagen secretion, but that it inhibits TGF-β-mediated elevation of collagen production in NIH 3T3 fibroblasts. Finally we explored that C184M suppresses TGF-β1 stimulation of NIH 3T3 cellular contractility.

II. Literature Review

1.0 Cardiovascular Disease

Cardiovascular disease is the No. 1 worldwide killer of men and women, including Canada. In this country, someone dies from heart disease or stroke every seven minutes. Heart disease and stroke burden Canadian society with health care costs that are more than $18 billion every year (http://www.heartandstroke.com/site/c.ikIQLcMWJtE/b.3483991/k.34A8/Statistics.htm). Cardiovascular disease is a general term which is used for various myocardial and circulatory system diseases including ischemic heart disease, cerebrovascular disease (stroke), rheumatic heart disease, peripheral vascular disease, heart failure, and congenital heart disease. Ischemic heart disease or coronary artery disease is the prevalent form of cardiovascular disease in Canada (http://www.phac-aspc.gc.ca/cd-mc/cvd-mcv/cvd-mcv-eng.php), which is usually resulted from high concentration of low-density lipoprotein cholesterol and subsequent atherosclerosis [35]. Rupture of atheromatous plaques leads to the formation of coronary thrombus and consequence cardiac ischemia and myocardial infarction.

2.0 The pathology of myocardial infarction (MI)

Myocardial infarction (MI) is an irreversible myocardial necrosis due to inadequate blood supply to the infarcted area. Most myocardial infarctions are initiated by acute rupture of an atherosclerotic plaque and subsequent formation of a coronary thrombus. Coronary artery occlusion results in ischemic injures in cardiomyocytes including

cessation of aerobic metabolism, depletion of creatine phosphate, onset of anaerobic glycolysis, accumulation of anoxic metabolism products and subsequent functional defects such as depressed contractile activity and electrocardiographic changes, cessation of contraction, alterations in membrane potential and ultimately death of myocytes in the area which anatomically is supplied by this artery [36, 37]. Necrotic myocytes initiate an inflammatory reaction which results in resolution of the matrix debris and dead cells from the infarct site followed by activation of reparative pathways that ultimately result in wound healing and formation of scar. Infarct healing causes structural changes in the left ventricle termed "*ventricular remodeling*", a complex process which in turn results in dilatation, hypertrophy, and enhanced sphericity of the ventricle. These geometrical and architectural changes in ventricle structure impair ventricular function and finally lead to heart failure [3, 38].

3.0 Cardiac repair and remodeling following infarction

Following myocardial infarction, a highly regulated process of cardiac repair and remodeling occurs. Repair and remodeling processes can be divided into three overlapping phases including, inflammatory phase, proliferative phase and maturation phase [39]. Inflammatory phase initiates with the release of intracellular contents of necrotic cells that leads to upregulation of cytokines and chemokines and subsequent recruitment of leukocytes into the infarcted area[40, 41]. Infiltration of neutrophils, macrophages and monocytes into the injured myocardium is coincident with the increased expression of matrix metalloproteinases (MMPs) which degrade existing matrix and vasculatures and facilitate migration of leukocytes into the damaged area [42, 43]. Proteolytic and phagocytic

activities of infiltrated inflammatory cells remove matrix debris and dead cells from the infarcted site [44]. Monocytes differentiate into macrophages and secrete fibrogenic and angiogenic growth factors which are involved in the formation of highly vascularized granulation tissue, containing myofibroblasts[45-47]. In the proliferative phase, proinflammatory cytokine and chemokine synthesis is suppressed by transforming growth factor-β (TGF-β) and interleukin (IL)-10, while fibroblasts and endothelial cells infiltrate the wound [48]. Fibroblasts differentiate into myofibroblasts which are a major source of collagen secretion in healing myocardial infarcts[7, 49, 50]. During the infarct maturation phase, a collagen base scar is formed; [51] however the infarct scar remains populated by myofibroblasts for months and years after the initial infarct [52].

4.0 Cardiac myofibroblasts

During wound healing interstitial quiescent fibroblasts and bone marrow derived cells (BMDC) undergo a phenotypical modification and form contractile, proliferative, and hypersecretory myofibroblasts [53]. Myofibroblasts incorporate features of both fibroblasts and smooth muscle cells. These cells are fibroblastic in that they are spindle-shaped, have prominent cytoplasmic projections, and extensive rough endoplasmic reticulum (ER). Their smooth muscle features include longitudinal cytoplasmic bundles of microfilaments and multiple nuclear membrane folds [54]. Cardiac myofibroblasts express vimentin (but not desmin, known to be a key smooth muscle cell protein) as well as the embryonic isoform of smooth muscle myosin (Smemb), and high levels of α-smooth muscle actin (α-SMA) which is widely used as a universal marker of the myofibroblast phenotype [5, 52, 55]. α-SMA is essential for allowing the myofibroblasts to

modify and restructure collagen matrices in the interstitium of tissues [56]. These α-SMA-positive cells generate strong contractile forces which cause reduction of the damaged area [57, 58]. Spindle-shaped myofibroblasts appear in the myocardial scar between day 2 and 4 in rat, [59] and day 4 and 6 in human and persist for years after myocardial infarction in the human myocardial scars [52]. Myofibroblasts are a major source of extracellular matrix (ECM) proteins in the heart, and produce collagens I and III, which are the main components of myocardial infarct scar and normal matrix components of the healthy interstitium [7]. Furthermore, they secrete cytokines and growth factors, such as TGF-β [60] and endothelin [61], which regulate scar formation. Collagen accumulation in the scar, and more importantly in remnant heart, is due to persistent wound healing by myofibroblasts which results in cardiac stiffness, impaired cardiac performance, and subsequent systolic and diastolic heart failure.

5.0 TGF-β: pleiotropic and multifunctional cytokines

The TGF-β superfamily contains more than 60 members encoded in the eukaryotic genome, and they are known to participate in control of cell division, differentiation, migration, adhesion, organization and programmed cell death [62, 63]. This superfamily is composed of structurally related polypeptides and can be divided into two major groups the TGF-β/Activin group and the bone morphogenetic protein (BMP)/growth and differentiation factor (GDF) group [64].

To date, three mammalian isoforms of TGF-β have been identified (TGF-β 1, 2 and 3) which are encoded by distinct genes but signal through the same cell surface receptors and play critical independent roles during embryonic development and in a

wide variety of biological processes which regulate tissue homeostasis in adults [65, 66 67 68]. TGF-β1 is the prevalent isoform, whereas the TGF-β2 and TGF-β3 are expressed in a more limited spectrum of cells and tissues [69]. Knockout experiments in mice have demonstrated numerous non-compensated functions of the three TGF-β isoforms. Disruption of the TGF-β1 gene is lethal and almost 50% of animals die in uterus due to defective yolk sac vasculogenesis and hematopoiesis [70] Surviving TGF-β1 null mice do not exhibit gross developmental abnormalities but rather, undergo massive inflammatory reactions in various organs including heart and lung. TGF-β1 is also involved in the proliferation and extravasations of immune cell into the tissue [71]. In contrast to TGF-β1 null animals, TGF-β2 null mice exhibit prenatal mortality or an extensive range of developmental defects. These defective developmental processes include epithelial–mesenchymal interactions, cell growth, and extracellular matrix production resulting in cardiac, pulmonary, craniofacial, spinal, ocular, inner ear, and urogenital defects [72]. TGF-β3 knockout animals also exhibit defective epithelial-mesenchymal interactions resulting in cleft palate and abnormal lung development [73]. Thus this multifunctional superfamily is critical in a broad range of cell functions.

6.0 Key regulatory roles of TGF-β in cardiac repair

6.1 TGF-β induction and activation in cardiac injury

Members of the TGF-β family are markedly expressed in the infarcted myocardium and plays pivotal roles in wound healing of infarct area, cardiac repair and remodeling [13, 15, 74, 75]. All three isoforms of TGF-β are induced in the damaged area but they demonstrate distinct patterns of expression. TGF-β1 and β2 show early upregulation,

whereas TGF-β3 demonstrates delayed and prolonged expression [76, 77]. TGF-β is released from different cell types including lymphocytes, extravasated platelets, activated macrophages, injured myocytes, fibroblasts and myofibroblasts. Infiltrated platelets are the major producer of TGF-β during early stage of wound healing, whereas macrophages and myofibroblasts may be responsible for the sustained upregulation of TGF-β during the proliferative phase of healing [78-82].

TGF-β is produced as a precursor which undergo a proteolytic modification to produce the active forms [83 84]. The mature form of TGF-β is a homodimer of two 12.5 kDa polypeptides, which is able to interact with cell surface receptors and activate subsequent signal transduction pathway [85 86]. Protease activity of MMP2, MMP9 and plasmin play a key role in the activation of TGF-β [87-89]. Furthermore, expression of thrombospondin (TSP)-1 in the infarct border zone and production of reactive oxygen species and a mildly acidic environment are also capable of inducing TGF-β activation [90-92]. Bioactive TGF-β is released 3-5 hours following reperfusion to the ECM of the infarct and contributes to the inflammatory phase of healing [93].

Evidence indicates that TGF-β is localized in the site of ischemia and the surrounding tissue [94]. For example, Smad2, -3 and -4 mediators of TGF-β signaling pathway are upregulated in infarct zones, whereas inhibitory Smad7 is suppressed in healing infarct. These changes may potentiate cardiac fibrosis in the remodeling myocardium [95, 96].

6.2 The role of TGF-β in cardiac repair and remodeling following myocardial infarction

The pleiotropic and multifunctional effects of TGF-β predicate its usefulness in the transition from inflammation to fibrosis during cardiac healing and remodeling of the left ventricle following infarction [97]. Despite the early effects of TGF-β, including the recruitment of monocytes into the damaged area in canine heart, TGF-β1 attenuates leukocyte adhesion to the endothelium and inhibits transendothelial migration of neutrophils [98-100]. In addition, it suppresses the proinflammatory cytokine and chemokine production by activated macrophages and promotes resolution of inflammation [101, 102]. Massive inflammatory responses in TGF-β1 deficient mice confirm the anti-inflammatory effects of TGF-β1 and its roles in immune cells homeostasis [103]. Furthermore, TGF-β1 is also associated with development of tissue fibrosis through its inhibitory effects on matrix metalloproteinase (MMP) expression and upregulation of tissue inhibitors of MMPs (TIMPs) [104, 105]. TGF-β1 is known to induce the phenotypical conversion of fibroblasts to myofibroblasts, and markedly enhances ECM protein synthesis, including collagen types I and III, which leads to formation of permanent fibrotic scar [106, 107]. Due to potent actions of TGF-β1 in ECM metabolism and cardiomyocytes hypertrophy, it is known as a crucial mediator in ventricular remodeling and subsequent heart failure after infarction [108].

6.3 TGF-β signaling pathway in fibrosis

TGF-β transduces its signal from membrane to nucleus through the interaction of type I (TβRI) and type II (TβRII) receptors and their downstream effectors [109 110]. TGF-β

signaling pathways include Smad-dependent and -independent pathways. The Smad-dependent pathway is linked to ECM protein gene expression [111] and is initiated by the binding of bioactive TGF-β to type II transmembrane serine-threonine receptors. Type II receptors phosphorylate residues on Type I which in turn phosphorylate cytosolic receptor-regulated Smad (R-Smad) proteins. R-smad proteins (Smad2 and Smad3) form a complex with co-mediator Smads (Co-Smad) such as Smad4 and then translocate to the nucleus, where with other transcriptional factors, corepressors and coactivators they regulate the expression of target genes, including collagen [112 113] (Figure 1).

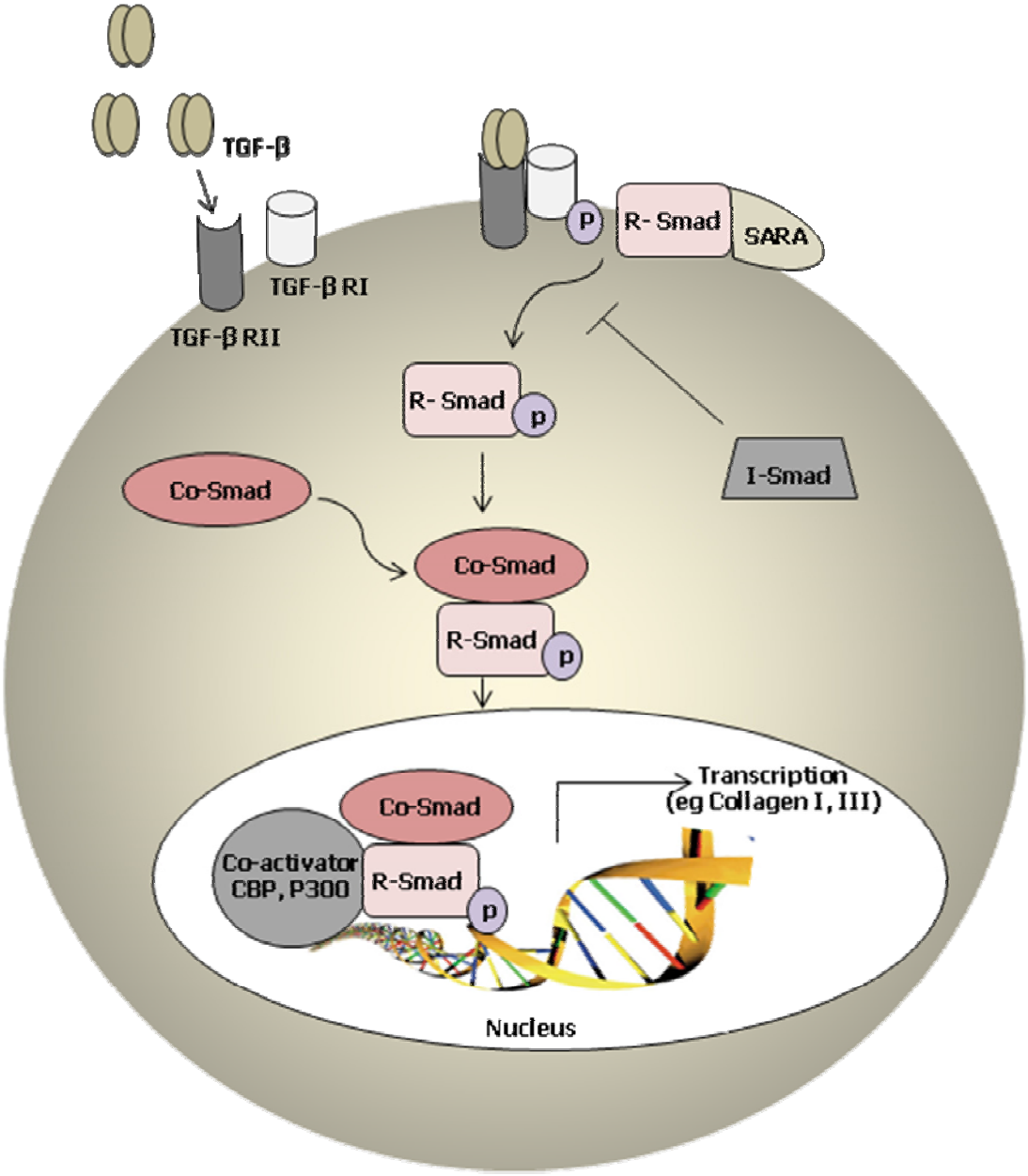

Figure 1. TGF-β/Smad signaling pathway. This depiction of the signaling pathway illustrates how TGF-β exerts its effects by signaling through Smad proteins, which then allows the transcription of specific target genes such as collagen.

7.0 Smad proteins

Mother against decapentaplegic, or MAD, was the first mediator of TGF-β signaling and was discovered in *Drosophila* [114] [115]. Subsequently, three proteins in *Caenorhabditis elegans*, Sma2, Sma3, and Sma4, which shared strong homology to *Drosophila's* MAD, were discovered and found to be involved in TGF-β signal transduction [116]. Human tumor suppressor DPC4 (deleted in pancreatic carcinoma, locus 4) was reported as the first vertebrate MAD homolog in 1996 [117]. Since then, the number of vertebrate family members has increased and the unified name "Smad" was given to them to indicate the homology to MAD and Sma proteins [118]. To date 9 distinct Smad proteins have been discovered. These intracellular proteins are associated with the propagation of TGF-β superfamily signals from the cell surface to the nucleus [119] [120]. Smads range from about 400 to 500 amino acids in length and can be functionally divided into three distinct subfamilies: (i) the receptor-regulated Smads (R-Smads) including Smad1, Smad2, Smad3, Smad5, and Smad8, (ii) the co-mediator Smads (Co-Smads), including Smad4 in mammals and Smad4β (also known as Smad10) in *Xenopus*, and (iii) the inhibitory Smads (I-Smads), including Smad6 and Smad7 [121] [122].

7.1 Receptor regulated Smads (R-Smads)

R-Smads are divided into two subgroups: i) Smads 2 and 3 which are activated by TGF-β1/Activin superfamily signals; ii) Smads 1, 5, and 8 which belong to the BMP-responsive group [123]. Most Smads are composed of two conserved MAD homology (MH) domains at the amino (MH1) and carboxyl (MH2) termini, which are separated by a proline-rich linker region of varying length [124]. In addition R-Smads have Ser-Ser-X-Ser

(SSXS) motifs in their C-terminal segment which are phosphorylated by type I receptors [125] [126]. Smad proteins bind to DNA through the MH1 domain while the MH2 domain is involved in differential association with a wide variety of proteins [127] [128]. R-Smads are anchored as dimers to the plasma membrane, through Smad anchor for receptor activation (SARA) proteins, and MH1 and MH2 domains are physically associated with each other [129]. The interaction between the MH1 and MH2 is disrupted upon receptor activation and phosphorylation of R-Smads.

7.2 Co-mediator Smads (co-Smads)

Smad4 is the only member of the Co-Smad subfamily in mammals. It was originally isolated as the product of the tumor suppressor gene DPC4 [130]. Smad4 is an intracellular protein that is structurally similar to R-Smads. It is composed of highly conserved MH1, MH2 domains at the N- and C-termini, respectively, and an intervening non-conserved linker region. As Smad4 lacks the SSXS sequence at the very most C-terminal part, it cannot undergo phosphorylation by type I receptors. Instead it can form a heteromeric complex with R-Smads upon activation of receptors and translocate from the cytoplasm to the nucleus [131] [132]. In the nucleus Smad4 stabilizes the Smad DNA-binding complex and also recruits transcriptional co-activator to regulate the expression of target genes [133]. Cycles of Smad4 monoubiquitination and deubiquitination regulate the formation of Smad complexes. Smad4 interacts with Ectodermin (Ecto) or TIF1γ in the nucleus which leads to its monoubiquitination and dissociation from R-Smad [134]. Activity of the deubiquitinase FAM/USP9 in the cytosol results in deubiquitination of Smad4 and its return to the Smad signaling pool [135].

7.3 Inhibitory Smads (I-Smads)

Smad6 and Smad7 belong to the inhibitory Smad (I-Smad) subfamily that are known to antagonize TGF-β1 signaling [121] [136] [137] [138]. I-Smads are structurally similar to R-Smads except that they have a poorly conserved MH1 domain. Expression of I-Smads is induced by different extracellular stimuli, including TGF-β1/Activin and BMPs [139]. I-Smads negatively regulate TGF-β1/BMP signaling through several mechanisms. First, they act as pseudosubstrates for TβRI and BMP type I receptors and interfere with receptor activation of corresponding R-Samds [140] [141] [142]. Second, Smad7 recruits protein phosphatase1 to inactivate type I receptors [143] and also functions as an adaptor protein to recruit E3 ubiquitin ligases, Smurf1 and Smurf2, to degrade TβRI [144] [145]. Smad6 inhibits BMP/Smad1 signaling by competing with Smad4 for binding to receptor-activated-Smad1 and producing an inactive Smad1-Smad6 complex [146]. Smad6 cooperates with Smurf1 and induce ubiquitination and degradation of BMP type I receptors, Smad1 and Smad5 [147]. Finally, I-Smads function in the nucleus and negatively regulate TGF-β1/BMP signaling. Smad7 competes with receptor-activated R-Smads in the nucleus for binding to DNA. This DNA-binding activity of Smad7 is mediated by the MH2 domain [148], while R-Smads bind to DNA through their MH1 domain [127] [149]. Smad6 represses transcription by recruiting transcriptional corepressors, such as histone deacetylase, CtBP, and homeobox (Hox) c-8 [150] [151] [152].

8.0 Ski family

The first member of the Ski gene family, v-Ski was originally identified in the avian Sloan-Kettering retrovirus which causes oncogenic transformation of chicken

embryo cells [153]. The Ski family consists of v-Ski, c-Ski, three spliced variant of SnoN (ski-related novel gene) and two recently identified members, Fussel-18 (Functional Smad suppressing element on chromosome 18) and Fussel-15[154]. Despite wide expression of Ski and SnoN in all adult tissues, expression of Fussel-15 and Fussel-18 is limited to neural tissues. These new members share high homology with Ski and SnoN and play an inhibitory role in the expression of TGF-β responsive genes through interaction with R-Smad proteins [155, 156]. Ski and SnoN structurally are composed of a DHD (Dachshund homology domain) domain in their N-terminal region [157, 158], a Smad4 binding domain (SAND)[159] and a less conserved C terminal region [160].

8.1 Biological Function of Ski

Data show that Ski is expressed in all embryonic and adult tissues in the mouse and plays important role during embryonic development and adulthood [161]. Ski knock-out mice show decreased skeletal muscle mass, craniofacial and skeletal abnormalities and pups die prenatally [162]. In humans, the 1p36 syndrome is a result of monosomy in the 1p36.3 region of chromosome 1, which contains the Ski gene. This genetic disorder phenotypically resembles that of the Ski knock-out mouse phenotype, and suggests that disruption of the Ski gene may causes this syndrome [163, 164]. Experimental evidence has indicated the role of ski protein in adult tissues, such as induction of muscle specific genes expression [165] and the regulation of Schwann cell proliferation and myelination [166]. *In vitro* studies indicated the involvement of Ski in the growth and differentiation of hematopoietic cells [167, 168]. Furthermore, Ski expression is changed during wound healing [169], liver regeneration [170], and different types of cancers [171-173].

8.2 Molecular mechanism of Ski in TGF-β signaling pathway

Ski is a co-repressor which can be recruited to TGF-β responsive promoters through association with Smad2, Smad3 and Smad4 [174-177]. Ski negatively regulates TGF-β1/Activin and BMP signaling pathways through the disruption of active heteromeric complexes formed between Co-Smad and R-Smads [178]. In addition Ski can interact with other co-repressors, like N-CoR, HIPK2 and mSin3A, and recruit histone deacetylase complex to the target TGF-β1/BMP- responsive promoters and repress transcription of corresponding genes [179] [180] [181]. Ski also competes with p300/CBP, a transcriptional co-activator of Smads, and recruits histone deacetylase complex to target genes and repress transcription [182] [183].

9.0 C184M

In 1999, three related cDNAs were discovered in developing mouse brain; named C184S, C184M, and C184L which encode two unrelated proteins. C184S and C184M are the 3'-end, and the 5'-end segments of C184L respectively. C184L has open reading frames (ORF) 1 and 2 which correspond to C184S and C184M, respectively [184]. C184S is a homologue of human autoantigen p27 [185], while C184M is a homologue of mammary tumor virus receptors [186].

9.1 Biological function of C184M

C184M is a cytosolic protein of 189 amino acids, and is known to suppress the activity of promoters containing Smad-binding sites, and TGF-β-induced growth

inhibition of mink lung Mv1Lu cells [187]. Previous studies have shown that C184M interacts with C-terminal coiled coil region of Ski through its leucine-rich motif and sequester Ski inside the cytosol. Consistent with this finding, Ski accumulates in the cytosol of hepatocytes that express high levels of C184M. C184M-Ski complex in turn, inhibits nuclear translocation of Smad2 and represses expression of TGF-β responsive genes. There seems to be no direct interaction between C184M and R-Smads and, cooperation of C184M and Ski causes sequestration of R-smad inside the cytosol [188].

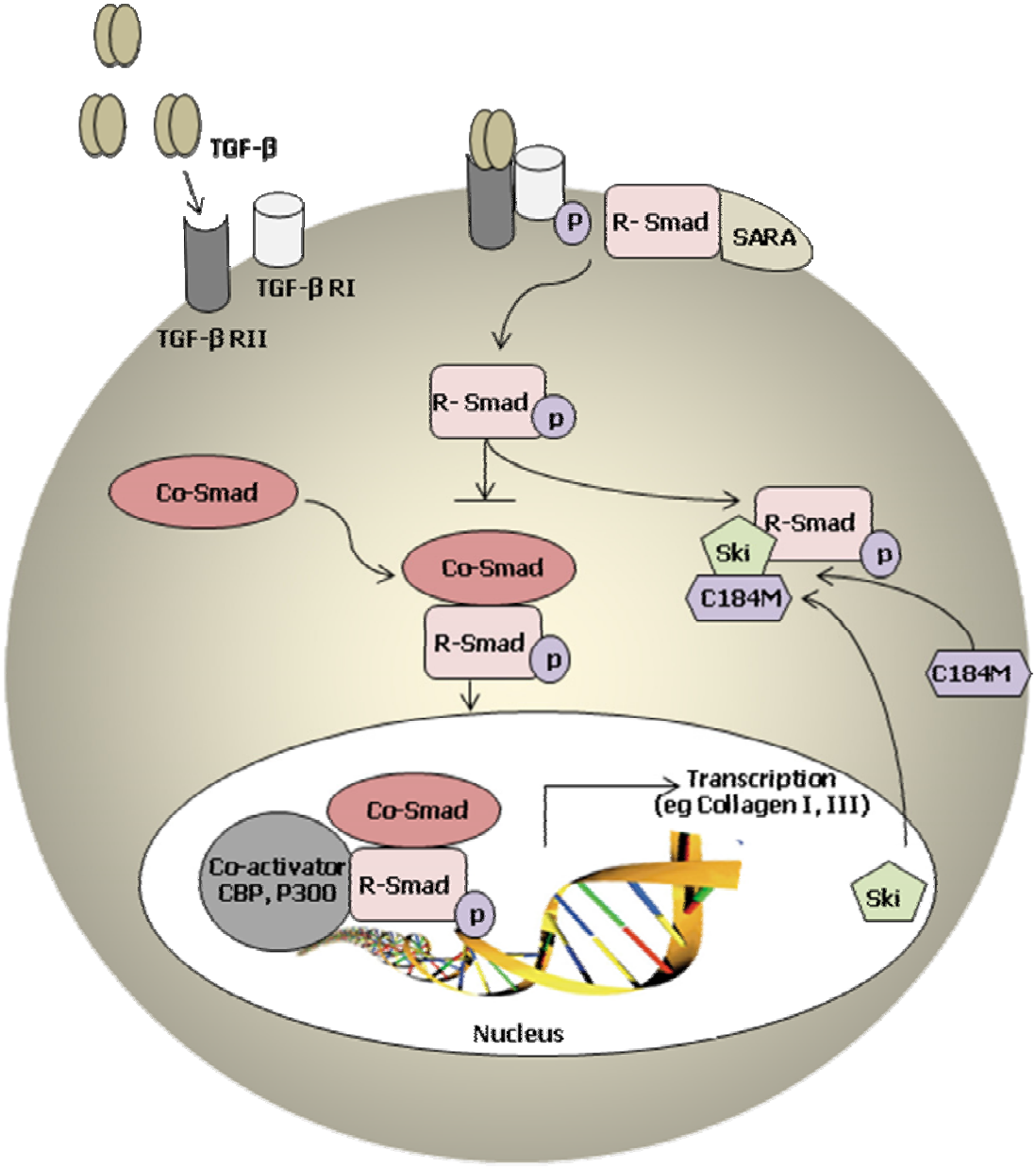

Figure 2. Inhibitory effect of C184M in TGF-β signaling pathway. This schematic shows the inhibitory effect of C184M in TGF-β signaling pathway through association with Ski and sequestering R-Smads inside the cytosol.

III Statement of Hypothesis

Previous studies have shown that C184M binds to the coiled-coil region of Ski via its own leucine-rich motif. This Ski-binding partner increases expression of Ski protein and suppresses the activity of promoters containing Smad-binding sites. Association of Ski and C184M is involved in retention of R-Smads, which are downstream mediators of TGF-β, in the cytosol. In addition, C184M abrogates the TGF-β-mediated growth inhibition of mink lung Mv1Lu cells [189]. As C184M is involved in regulation of the TGF-β signaling pathway, and TGF-β is a major mediator in fibrosis, we have explored the role of C184M in TGF-β mediated cell function in fibroblasts. **We hypothesize that overexpression of C184M would abrogate NIH 3T3 fibroblasts contractility and collagen secretion via its interactions with Ski and R-Smads, respectively.**

IV Materials and Methods

1.0 Materials and Reagents

Culture media (Dulbecco's Modified Eagle Medium, DMEM, DMEM/F12, and Minimum Essential Medium, SMEM), antibiotics (penicillin and streptomycin), fetal bovine serum (FBS) and TrypLE™ Express were purchased from Invitrogen. N-terminal propeptide of type I procollagen (P1NP) enzymoimmunoassays (EIA) was obtained from Immuno Diagnostic System (IDS). Culture dishes, multi-well plates and flasks were from Fisher Scientific. Collagen type I solution for gel contraction assays was purchased from Stem Cells Technologies. RT-PCR Green Master Mix was supplied by Promega and qPCR iQ™ SYBR® Green Supermix was obtained from Bio-Rad. Protein assay reagents (Bicinchoninic acid and copper II sulphate) were ordered from Sigma-Aldrich. Polyvinylidene difluride (PVDF) blotting membrane were acquired from Roche Applied Sciences. Pre-stained molecular weight ladder SeeBlue2 and MagicMark™ was supplied by Invitrogen. Chemiluminescence (ECL and ECL Plus). Clean-Blot® IP Detection Reagent was purchased from Thermo Scientific. Recombinant Human TGF-β11 was received from R&D Systems. Surgical Blades were purchased from Becton-Dickinson Acute Care. Alexa Fluor conjugated secondary antibodies were acquired from Molecular Probes. Anti-mouse Ig Texas Red-conjugated antibody was from Amersham Pharmacia Biotech. SlowFade® Gold Antifade Reagent was ordered from Molecular Probes. Primary antibodies specific for Ski and Smad3 were obtained from Upstate, β-tubulin from Abcam, and C184M was a gift from Dr. Shunsuke Ishii, laboratory of Molecular Genetics, RIKEN Tsukuba Institute, 3-1-1 Koyadai, Tsukuba, Ibaraki 305-0074, Japan.

2.0 Methods

2.1 Isolation and culture of rat cardiac fibroblasts and myofibroblasts

Ventricular fibroblasts were isolated from adult male Sprague-Dawley rats of 175-200 grams as previously described [190, 191]. Briefly, rats were anesthetized with a 1:10 Ketamine/Xylazine mixture using 0.1 ml/100 gram body mass. Rats also received a heparin injection in the femoral vein to prevent blood clotting. Hearts were excised and subjected to Langendorff perfusion at a flow rate of 5 ml/minute at 37^{o}C first with DMEM/F12, and then SMEM for 5 minutes each, followed by perfusion with recirculated SMEM containing 0.1% collagenase for 20-25 minutes. Digested hearts were then transferred to a dish containing 0.05% collagenase in SMEM. Using forceps, hearts were shredded into smaller pieces then incubated at 37^{o}C and 5% CO_2 for 15 minutes. Released cells were collected by centrifugation at 2000 rpm using bench model centrifuge Beckman TJ-6, for 7 minutes and resuspended in DMEM/F12 supplemented with 10%FBS, 0.1 mM ascorbic acid, 100 U/ml penicillin and 100 μg/ml streptomycin. Cells were plated and allowed to adhere for 2 hours, and then washed twice with 1x phosphate buffered saline (PBS) to get rid of all non-adherent cells and myocytes, and then were maintained in 10% FBS DMEM/F12. Cells were confluent enough to passage after 4 days and we used passage 1 (P1) cells for our experiments unless otherwise noted.

2.2 pMXIE-EGFP and FLAG-C184M-EGFP retrovirus preparation and titration

Phoenix-ECO cells were seeded at $2x10^7$ cells/T175 flask and allowed to grow overnight to ~ 70% confluency. Retroviral DNA constructs were transfected into the cells with calcium phosphate (Ca_2PO_4) as follows: 5 minutes prior to transfection the media of cells was replaced with 25 ml of 10% DMEM media containing 100 µl chloroquine (10 mM). 12.5 µg of target DNA was brought to a volume of 960 µl with sterile DDW and was kept on ice for 10 minutes. 133 µl $CaCl_2$ 2M was then added dropwise into the diluted DNA and the mixture was kept on ice for 5 minutes. 1.11 ml of 2x HBS was added dropwise to the mixture while mixing thoroughly and the solution was kept on ice for an additional 20 minutes. Finally the HBS/DNA solution was gently added dropwise onto the media and quickly by spreading across cells in the media. Cells were then transferred into a 37 ^oC, 5% CO_2 incubator and the plates rocked forward and backward a few times to evenly distribute DNA/CaPO4 complexes. The media was replaced with 40 ml 10% DMEM media after 6-8 hours. The cells were then transferred into a 32 ^oC, 5% CO_2 incubator and allowed to produce virus for 3 days. The media containing virus was collected in a 50 ml tube, centrifuged using bench model centrifuge Beckman TJ-6, at 1,200 rpm for 5 minutes to pellet cell debris, filtered using a Millipore Steriflip filter, and finally transferred into polypropylene copolymer tube and spun at 6,250 rpm (600 g) where RCF = 1.12r x $(rpm/1000)^2$, and r = 137 mm (rotor JA-14), using Beckman J2-HS centrifuge for 90 minutes at 4 ^oC. The supernatant was poured off, leaving the left-over drops in the bottom of the tube (left-over volume ~250 µl). One hundred fifty µl of fresh media was added to the pellet to bring the volume to 400 µl and the virus pellets were

resuspended in the media and kept in -80 ^{o}C freezers. Four hundred µl of virus was produced from each flask, which was considered equal to 100X concentrated (i.e. 40 ml→ 400 µl). NIH 3T3 fibroblasts were used to titer the retroviruses. 5x10^4 cells/well were plated in a 24-well dish and allowed to grow overnight. 1x and 0.1x concentration of viruses were prepared by adding 10% media up to 297.6 µl and 2.4 µl of polybrene. The cell media was removed before adding 250 µl of the prepared 1x and 0.1x virus. The cells were then incubated for 2 hours at 37^{o}C. The cell media was changed after 2 hours infection and replaced with fresh 10% media. The cells were allowed to grow for 3 days before being harvested. As infected cells express EGFP protein which fade due to photobleaching, all harvesting processes were done in dark. The cells were washed once with 1x PBS, trypsinized with 0.2 ml TrypLE^{TM} Express and received 0.8 ml 10% media to dilute TrypLE^{TM} Express. All cells were then collected in a flow tube, diluted with 3ml 1x PBS and spun down using bench model centrifuge Beckman TJ-6 for 7 min at 1,200 rpm. The supernatant was poured off, leaving the left-over drops in the tube. The tube was then capped and tapped 6-10 times on the bench to collect all the remaining of supernatant at the bottom of tube. The cells were then re-suspended and fixed with 200 µl of 2% Paraformaldehyde (PFA) and examined using Fluorescence Activated Cell Sorting (FACS) machine to quantify the percentage of infected cells expressing EGFP. The following equation was used to calculate the viral titer (virus particle/ml).

Virus (vp/ml)= The number of cells x % EGFP positive x 4 x dilution factor x 100

2.3 Optimization of FLAG-C184M-EGFP retrovirus Multiplicity Of Infection (MOI) and infection of P0 fibroblasts using FLAG-C184M-EGFP and pMXIE-EGFP retroviruses

Optimal MOI's for C184M-EGFP retroviruses were determined by infecting P0 fibroblasts with different MOIs of 25, 50, 100, 150, 200, 250, 300, 600 and 1,000 and measuring the percentage of infected cells using FACS machine. An MOI of 150 vp/cell was the optimal MOI for FLAG-C184M-EGFP retroviruses. Optimal MOI for pMXIE-EGFP which had been determined previously in our lab, was the same as FLAG-C184M-EGFP retroviruses. P0 fibroblasts in a 24-well plate were infected at 20-40% confluency with the optimal MOI for 6-12 hours. Cells were subsequently passaged and used for immunocytochemistry studies.

2.4 Immunocytochemistry

P0 fibroblasts were infected with retrovirus as explained in section 2.3 and then were passaged to obtain P1 cells for immunocytochemistry studies. P1 cells were seeded onto the coverslips and allowed to adhere overnight. The cells were starved for 24 hours to arrest the growth and then stimulated with TGF-β1 (10 ng/ml) for a further 24 hours. The cells were washed 3 times with cold 1x PBS, fixed in 4% paraformaldehyde for 15 minutes, washed once with cold 1xPBS, permeablized with 0.1% Triton-X-100 in 1xPBS for 15 minutes. Cells were then blocked in 1x PBS containing 10% Bovine Serum Albumin (BSA) for 30 minutes, and then incubated overnight at 4 ^{o}C with rabbit-anti Smad3 or rabbit- anti C184M primary antibodies. Both antibodies were diluted in 1x PBS containing 1% BSA with ratio of 1:500 for Smad3 and 1:200 for C184M. Cells were then

incubated with goat anti-rabbit secondary antibody conjugated with Alexa Fluor 568, in the dark at room temperature for 2 -3 hours. Alexa Fluor 488 anti-EGFP was incubated with the cells for 2-3 hours at room temperature to enhance the EGFP signal following a 3 times washing cycle with 1x PBS. All Alexa Fluor conjugated antibodies were diluted in 1x PBS containing 1% BSA at a ratio of 1:700. The cells were then subjected to another washing cycle with 1x PBS, then dried well and mounted on slides with SlowFade® Gold Antifade Reagent containing DAPI. Slides were observed under a microscope (Nikon) equipped with epifluorescence optics. Epifluorescent images were photographed at 1000X magnification using appropriate filters.

2.5 Infection of P1 myofibroblasts using LacZ, Smad3 adenoviruses

P1 myofibroblasts were seeded in 100 mm petri dish and allowed to adhere overnight. Cells were starved for 24 hours and then at 80% confluency were infected for further 24 hours with Smad3 and LacZ adenoviruses with MOI of 10 and 100 (vp/cell) respectively. The optimal MOI's were determined previously in our laboratory.

2.6 Protein isolation and Protein assay

Cells from the different preparations were washed 2 times with cold PBS and lysed in 120 µl RIPA buffer (PH 7.6, 150 mM NaCl, 0.5% deoxycholate, 0.1% sodium dodecyl sulfate (SDS), 1.0% nonidet P-40 (NP-40), 50 mM Tris) containing 1x protease inhibitor cocktail (Sigma Aldrich Canada Ltd) and phosphatase inhibitors (10mM NaF, 1 mM Na_3VO_4 and 1 mM EGTA). The cells were scraped and collected into microcentrifuge eppendorf tubes, kept on ice for 1 hour, and then sonicated 3 times for 5 seconds each.

The cell lysate was centrifuged at 14,000 rpm using Eppendorf 5415C Micro Centrifuge for 15 minutes at 4^{o}C and then the supernatant was collected and stored at -20^{o}C. Total protein concentration was measured using the bicinchoninic acid (BCA) method as previously described [192].

2.7 Western blot analysis

Laemmli loading buffer (125mM Tris-HCl PH 6.8, 2.5% SDS, 5% glycerol, 0.125% bromophenol blue and 5% 2-mercaptoethanol) was mixed with cell lysates at a ratio of 1:3 and boiled for 5 minutes. Equal amounts of protein samples (10-50μg) were loaded and separated on 8-12% SDS-polyacrylamide gel by electrophoresis (SDS-PAGE) alongside 15μl prestained low molecular weight markers. Separated proteins were electrophoretically transferred to polyvinylidene difluoride (PVDF) membrane at 175 V for 90 minutes and blocked with 10% skim milk in Tris-buffered saline with 0.2% Tween 20 (TBS-T) for 1 hour at room temperature. The membranes were then probed with primary antibodies for 1.5 hours at room temperature or at 4 ^{o}C overnight at dilutions of 1:1000 for C184M, β-Tubulin and Smad3 and 1:250 for Ski, in 1% skim milk in 0.2% TBS-T. Anti-rabbit and anti-mouse secondary antibodies tagged with horseradish peroxidase (HRP)-labeled or Clean-Blot® IP Detection Reagent were incubated with membranes at dilution of 1:10,000 and 0.1 μg/ml in 1% skim milk in 0.2% TBS-T respectively for 1 hour at room temperature. Protein bands were visualized by ECL or ECL Plus, according to the manufacturer's protocol, and developed on X-ray film. Equal loading of different protein samples was assessed by re-probing the same membrane for β-Tubulin.

2.8 Rationale and employment of the NIH 3T3 fibroblasts for contractility and collagen secretion studies

As the transfection of primary myofibroblasts remains a technically challenging undertaking, overexpression of a specific protein in these cells is more easily realized via the use of a retro- or adenoviral vector. As we experienced difficulty acquiring sufficient numbers of cells/plate with C184M overexpression in primary ventricular myofibroblasts using pMXIE retrovirus (and as a C184M adenoviral construct was not ready), we decided to use human embryonic kidney 293 (HEK 293) cells and mouse embryonic fibroblast cells (NIH 3T3) in the current experiments. It is understood that the rat and human primary cell studies will be carried out after this initial work.

2.9 NIH 3T3 fibroblasts Transfection using Lipofectamine™ 2000 Reagent

Mouse embryonic fibroblast cells (NIH 3T3) cells were plated at $8.8x10^5$ cells/100 mm dish using 10% medium and allowed to adhere overnight. The cells were subjected to transfection at 70-80% confluency with N-FLAG-pact-C184M plasmid, using Lipofectamine™ 2000 Reagent in serum and antibiotics free media. The ratio of DNA to Lipofectamine™ 2000 was 1: 2.5, using a total amount of DNA of 10 μg in a 100mm dish. Media was replaced with fresh media containing no antibiotics after 6 hours.

2.10 Reverse Transcriptase Polymerase Chain Reaction (RT-PCR) and Quantitative Polyperase Chain Reaction (qPCR)

Rat cardiac fibroblasts (P0), myofibroblasts (P1, P2), and NIH 3T3 fibroblast cell line were subjected to RNA isolation using the GenElute Mammalian Total RNA Extraction Miniprep Kit. Isolated RNA was assessed by spectrophotometry to measure the concentration and agarose gel electrophoresis. One µg of RNA was then reverse transcribed using Superscript III First-Strand Synthesis System to produce cDNA. This cDNA was examined using spectrophotometry and used as a template for RT-PCR and qPCR. RT-PCR was completed using Promega Master Mix, rat C184M specific Primers (5'-ATATGTCCCTGTTGTGCCAG-3' and 5'-AGGTTCCTCGTCATCAGACA-3') or mouse c-Ski specific primers (5'-CTGCGAGTGAGAAAGAGACG-3' and 5'-TTTTCGTGGCTGGATACAAG-3') [193] or GAPDH specific primers (5'-TGCACCACCAACTGCTTAGC-3' and 5'-GGCATGGACTGTGGTCATGA-3') (sequence obtained from Dr. Michael Czubryt) and 1 µl of cDNA as a template. RT-PCR was performed using the following thermocycler conditions : 1 minute denaturing at 95 ^{o}C, 1 minute annealing at 58 ^{o}C, and 1 minute elongation at 72 ^{o}C. There was an initial denaturation of 3 minutes at 95 ^{o}C and a final extension of 5 minutes at 72 ^{o}C. Rat C184M was amplified for 20, 25, 30 and 35 cycles, whereas the c-Ski was amplified for 35 and 40 cycles.

qPCR was conducted according to a two-step protocol. Optimal conditions for all investigated genes were established using iQ™ SYBR® Green Supermix (BIO-RAD). Twenty five µl of the reaction solution consisted of 50 ng, 20 ng, and 2 ng of the template for C184M, c-Ski and GAPDH samples respectively, 12.5 µl of iQ™ SYBR® Green

Supermix, and 1 µl of 10 µM of each primer. qPCR was completed using mouse C184M specific primers (5'-TTAACCTCGACTCTGCACTA-3' and 5'-ACAGTAGGAGAGACGTGAGC-3') and the same GAPDH and c-Ski primers used for RT-PCR. PCR amplification was performed as follows: pre-denature for one cycle at 95 °C for 3 minutes, 40 cycles at 95 °C for 10 seconds and 60 °C for 30 seconds, one cycle at 95°C and 55 °C for 1 minutes each and one cycle at 55°C for 10 seconds. Melting curve analysis was performed at 57–72 °C with 0.8 °C/s temperature transition.

2.11 Floating collagen gel contraction assay: NIH 3T3 fibroblasts contractility

Floating collagen gels were prepared by mixing 7 ml of cold collagen type I solution (3mg/ml) with 2 ml of 5x concentrated DMEM. The final volume of the solution was brought to 10 ml with sterile DDW after adjustment of the pH to 7.4, using 1 M NaOH. Six hundred µl of gel solution was placed into each well of a 24-well plate and incubated overnight at 37°C to solidify. $1x10^5$ NIH 3T3 fibroblasts were plated onto each well and allowed to adhere to the gel matrix overnight. The cells were then transfected with N-FLAG-pact-C184M plasmid as was explained in section 2.9 in serum free condition, and media was replaced with fresh serum-free media 6 hours after transfection. Twenty four hours post-transfection, cells were stimulated with TGF-β1 (10ng/ml) for 24 hours and TGF-β1 was replenished every 12 hours. The gel was cut away from the wall of the culture plate well with a surgical scalpel blade immediately after stimulation with TGF-β1 to allow movement. The gels were digitally imaged at 0 and 24 hours after TGF-β1 stimulation. Gel surface area was quantified using IDL Measure Gel software.

2.12 Procollagen type I N-Terminal Propeptide (PINP) enzyme immunoassay

Mature collagen is assembled from procollagen molecules containing terminal extension proteins called amino and carboxy procollagen extension propeptides. These propeptides are cleaved from both the N- and C-terminal ends of the procollagen molecule in equimolar concentrations during collagen synthesis. Thus, the quantification of N-terminal propeptide of type I procollagen (PINP) provides a reliable measurement of collagen synthesis. PINP concentration was examined using Rat/Mouse PINP EIA kit provided by Immuno Diagnostic Systems (IDS). NIH 3T3 fibroblasts were plated in 100 mm dishes and allowed to grow in 10% DMEM containing 0.1 mM ascorbic acid overnight. The cells were then subjected to transfection with N-FLAG-pact-C184M plasmid, in serum free condition, as was explained in Section 2.9 and media of cells was replaced with fresh serum-free media 6 hours post-transfection. After 24 hours of transfection media was again replaced with fresh serum-free media and cells were stimulated with 10ng/ml TGF-β1 for 24 hours. TGF-β1 was replenished every 12 hours. Media and cells were scraped from the culture dish, collected and homogenized through 5 freeze-thaw cycles. 5 µl of homogenized samples were examined using Rat/Mouse PINP EIA kit according to the manufacturer's instruction. OD of samples was read at 450 nm and used to calculate the amount of collagen from a standard curve.

2.13 Statistical analysis

All data were analyzed using Sigma Stat software (Point Richmond, CA) and are shown as mean ± standard error (SE). Significant differences between various groups were determined using one-way analysis of variance (ANOVA) and compared using the

Student–Newman-Keuls *post hoc* test. Significant differences among groups were defined as P ≤ 0.05.

V Results

1.0 Expression of C184M and c-Ski in cardiac fibroblasts (P0), myofibroblasts (P1 and P2) and NIH 3T3 fibroblast cell line

C184M is a novel c-Ski binding partner which was initially discovered in developing mouse brain [194]. To examine the expression of C184M and c-Ski RNA transcripts in primary cardiac fibroblasts (P0) and myofibroblasts (P1 and P2) and NIH 3T3 fibroblasts we used RT-PCR. Total RNA was isolated from P0 fibroblasts and P1 and P2 myofibroblasts and NIH 3T3 fibroblasts and converted into cDNA. RT-PCR was run at different cycle using the generated cDNA and specific C184M and c-Ski primers. RT-PCR products were resolved on a 1.5% agarose gel and images were obtained using a molecular imager Gel DOC XR+ system from BIO-RAD. GAPDH was used as a control to show the amount of expression of C184M and c-Ski RNA in the examined cells. Figures 3 and 4 depict the expression of C184M and c-Ski respectively, in fibroblasts (P0) and myofibroblasts (P1 and P2), while Figure 5 illustrates the expression of C184M and c-Ski in NIH 3T3 fibroblast cell line.

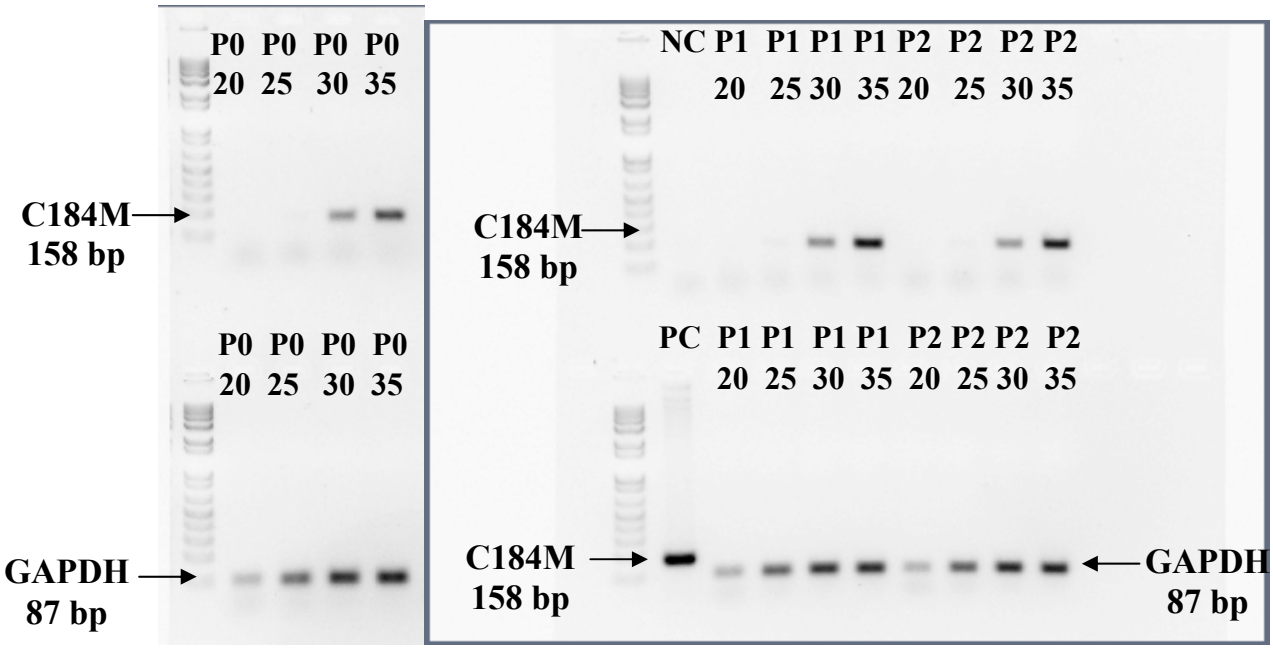

Figure 3. C184M mRNA transcript expression in fibroblasts and myofibroblasts using RT-PCR. RNA was isolated from 80% confluent fibroblasts (P0) and myofibroblasts (P1 and P2). Isolated RNA was used for reverse transcription PCR at different cycles (20, 25, 30, and 35). Amplified DNA was run on 1.5% agarose gel and bands visualized using molecular imager Gel DOC XR+ system from Bio-Rad. Negative control (NC) and positive control (PC)

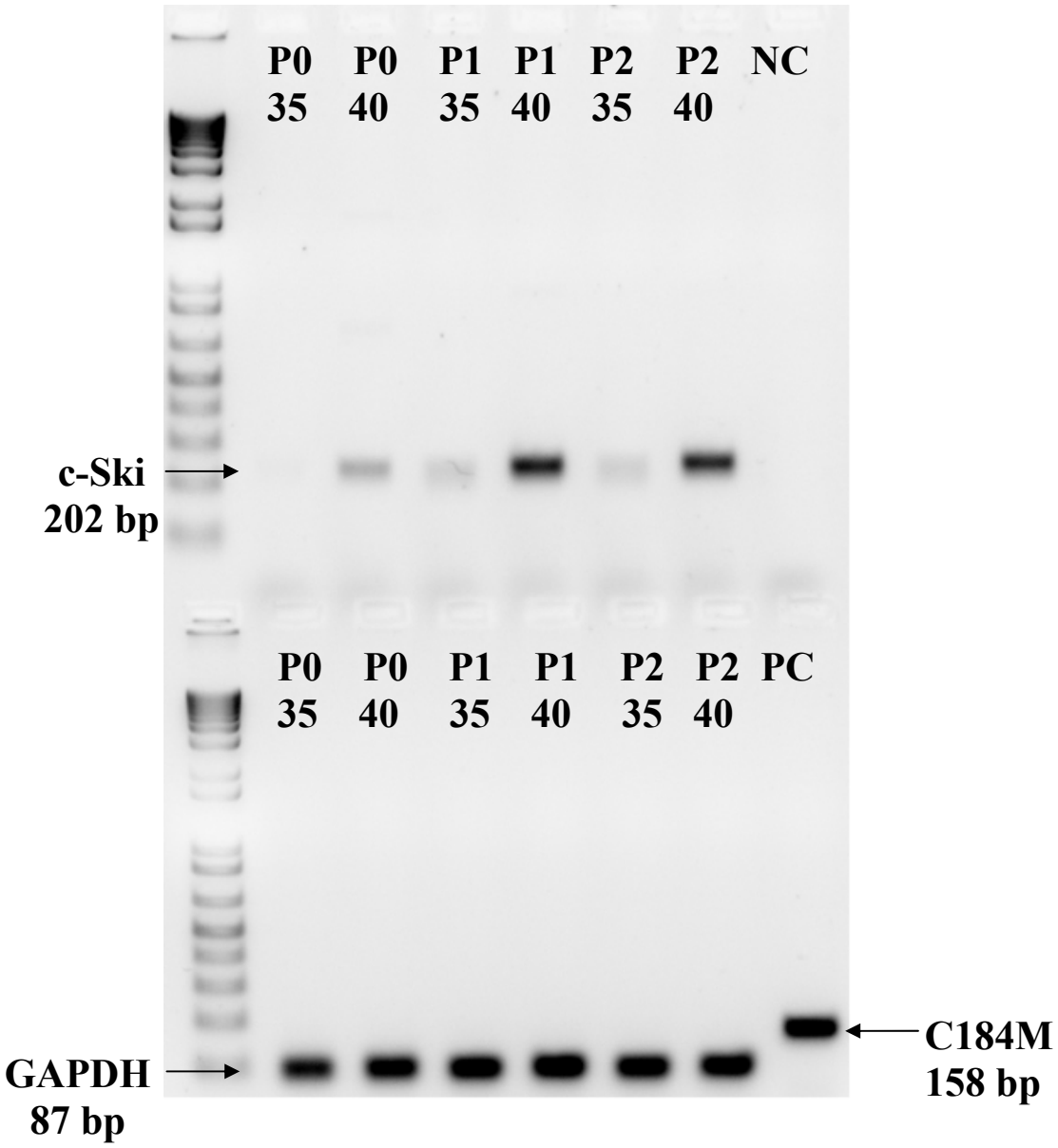

Figure 4. c-Ski mRNA transcript expression in fibroblasts and myofibroblasts using RT-PCR. RNA was isolated from 80% confluent fibroblasts (P0) and myofibroblasts (P1 and P2). Isolated RNA was used for reverse transcription PCR of different cycles (35and 40). Amplified cDNA was run on 1.5% agarose gel and bands visualized using molecular imager Gel DOC XR+ system from BIO-RAD. Negative control (NC) and positive control (PC)

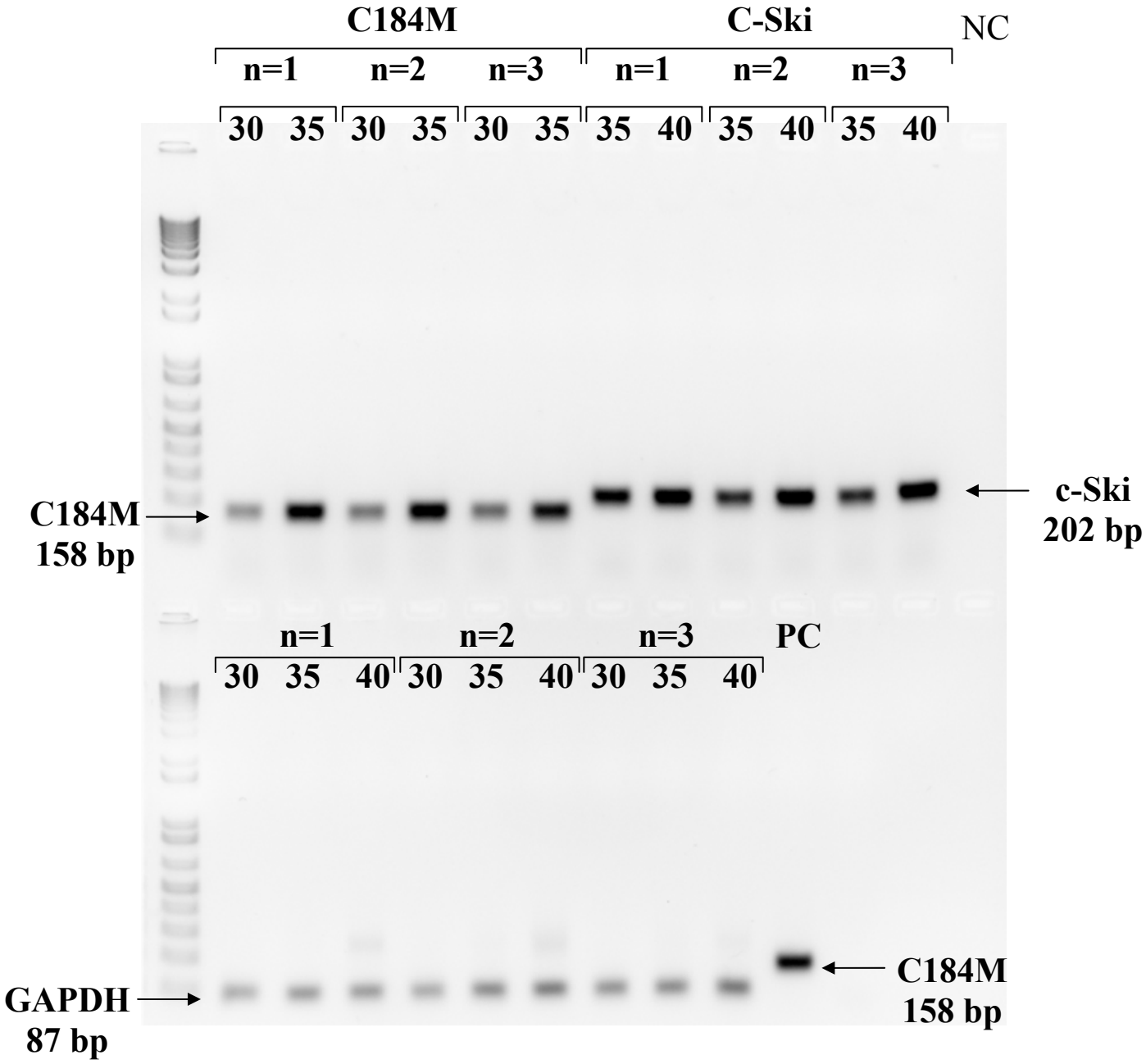

Figure 5. C184M and c-Ski mRNA transcript expression in NIH 3T3 fibroblasts using RT-PCR. RNA was isolated from 80% confluent NIH 3T3 fibroblasts. Isolated RNA was used for reverse transcriptase PCR at different cycles. Amplified cDNA was run on 1.5% agarose gel and bands visualized using molecular imager Gel DOC XR+ system from BIO-RAD. Negative control (NC) and positive control (PC)

2.0 Optimization of qPCR conditions for amplification of C184M, Ski and GAPDH mRNA expression

Expression of C184M and Ski mRNAs in cardiac fibroblasts (P0) and myofibroblasts (P1 and P2) and NIH 3T3 fibroblasts was demonstrated using reverese transcription PCR technique (Fig 1,2, and 3). In order to quantify the expression of these mRNA species in different conditions we need to use quantitative PCR (qPCR). qPCR or real-time PCR is an enhanced diagnostic tool which is highly suited for a wide range of applications, including mRNA expression analysis. Fluorescent monitoring of DNA amplification is the basis of this highly sensitive technique. We determined the best annealing temperature for all three mRNA species which was 60^{o}C. The standard curve for each mRNA species was constructed based on methodology employing known concentrations. Dilution series of 5 different concentrations were prepared in triplicate and were used to generate standard curves (Figures 6A, 7A, and 8A). All standard curves are valid, as the slope of them is between the acceptable range (-3.3 to -3.8) according to Qiagen real-time PCR handbook (critical factors for successful real-time PCR). We also determined the optimal amount of template in the reaction for C184M, Ski and GAPDH which are 50 ng, 20 ng, and 2 ng respectively (Figures 6B, 7B, and 8B). These optimal conditions can be used for future studies to quantify the expression of these mRNAs in different conditions.

A

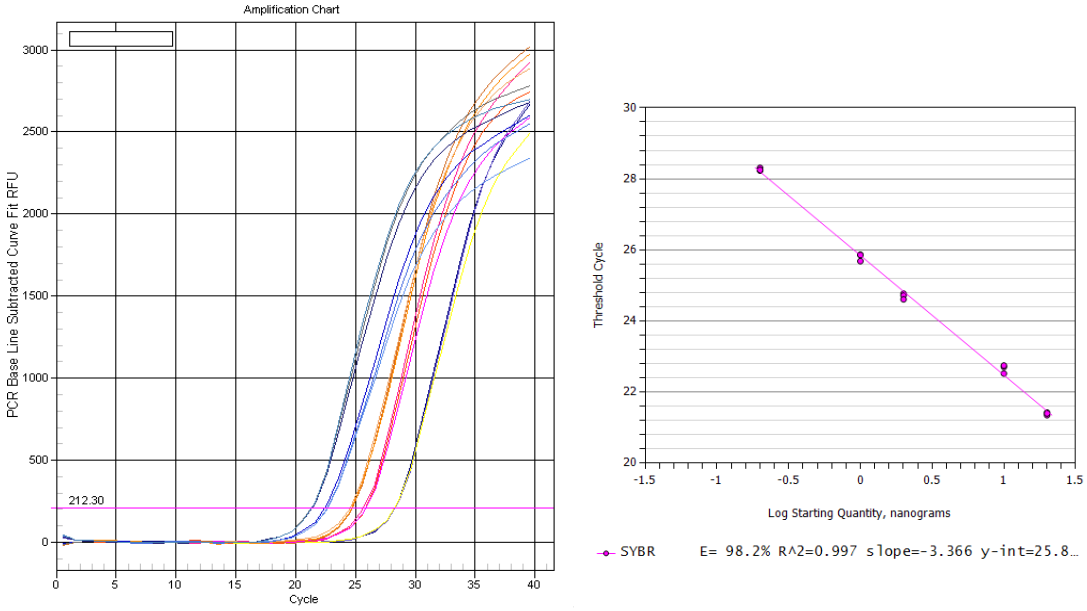

B

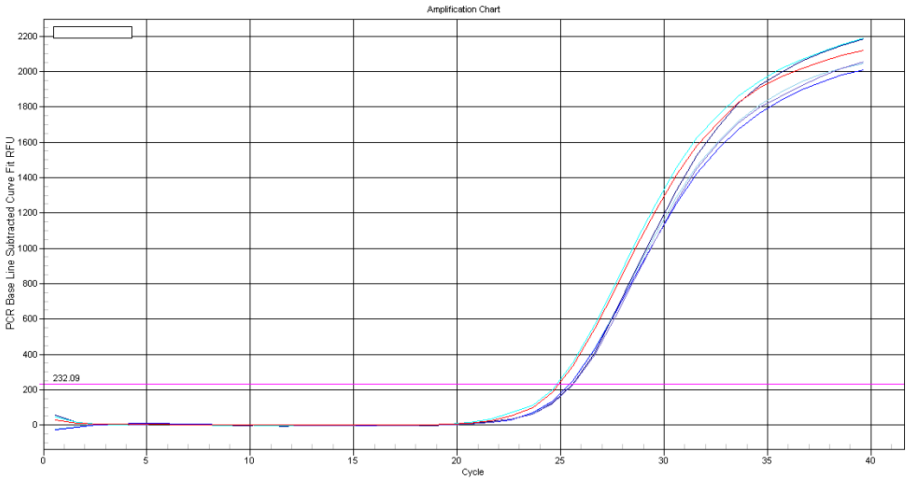

Figure 6. GAPDH mRNA standard curve and qPCR results using established optimal conditions with mRNA extracted from NIH 3T3 fibroblasts. Panel A: Constructed GAPDH standard curve. The slope of standard curve is -3.366 and efficiency of the reaction is 98.2%. **Panel B:** qPCR result for GAPDH using 2 ng of cDNA as a template.

A

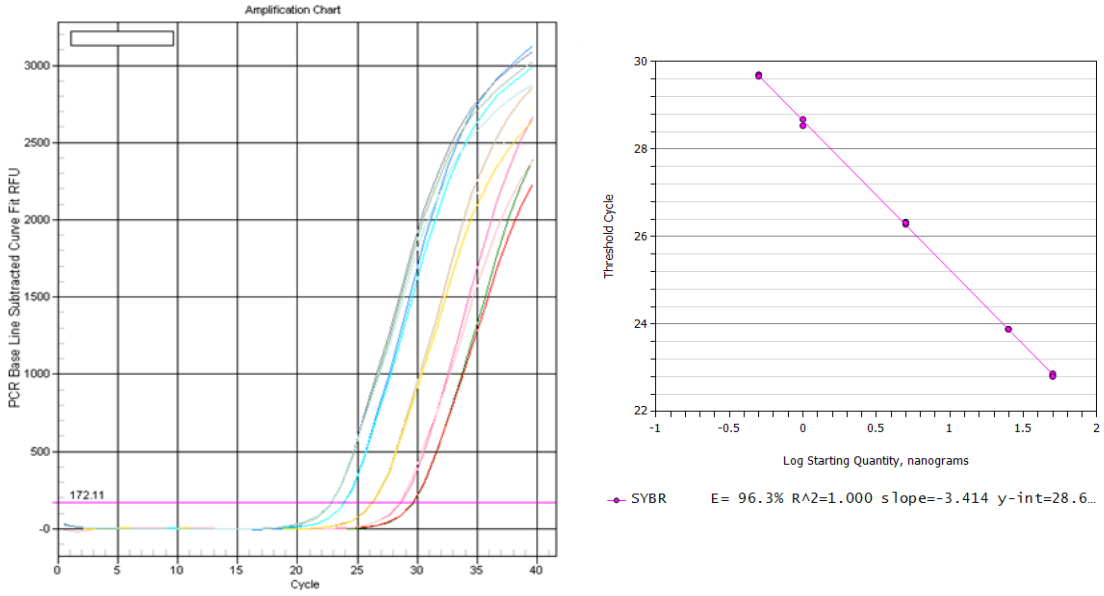

B

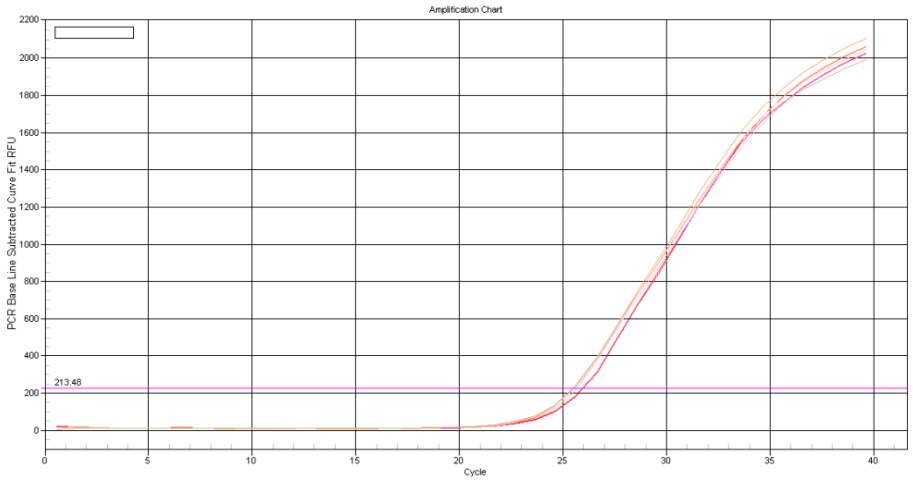

Figure 7. Ski mRNA standard curve and qPCR results using established optimal conditions with mRNA extracted from NIH 3T3 fibroblasts. **Panel A:** Constructed GAPDH standard curve. The slope of standard curve is -3.414 and efficiency of the reaction is 96.3%. **Panel B:** qPCR result for Ski using 20 ng of cDNA as a template.

A

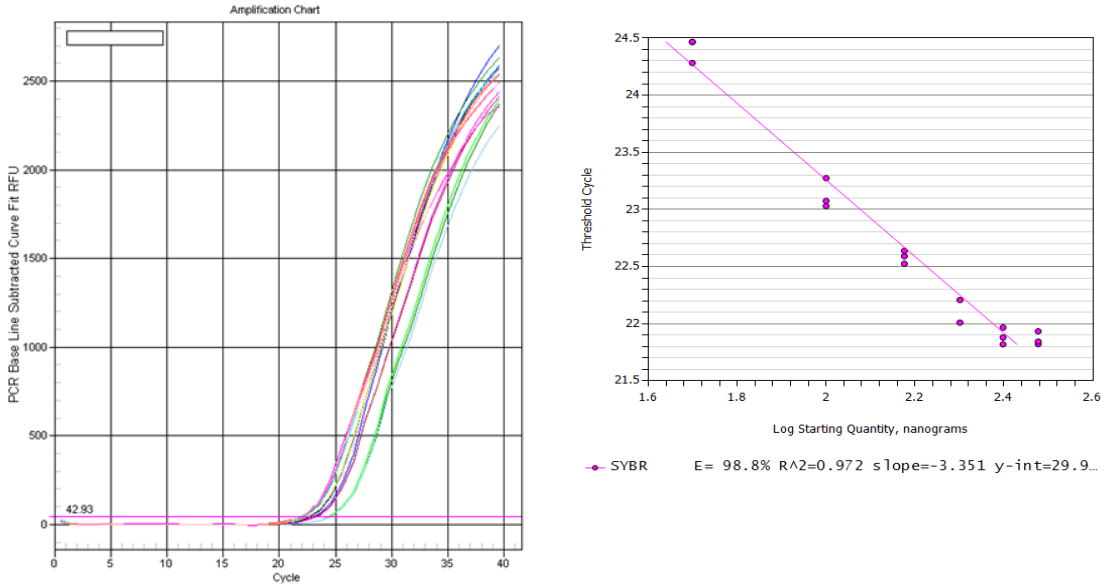

B

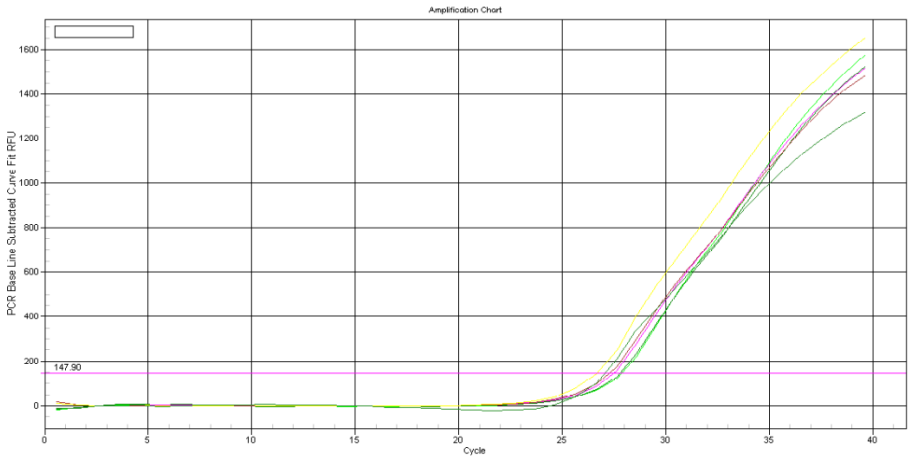

Figure 8. C184M mRNA standard curve and qPCR results using established optimal conditions with mRNA extracted from NIH 3T3 fibroblasts. Panel A: Constructed GAPDH standard curve. The slope of standard curve is -3.352 and efficiency of the reaction is 98.8%. **Panel B:** qPCR result for C184M using 50 ng of cDNA as a template.

3.0 Effect of TGF-β1 stimulation on the C184M expression

TGF-β1 affects a multitude of cell functions including proliferation, differentiation, migration, and apoptosis, and has been implicated as a key regulator of wound healing and extracellular matrix remodeling [195, 196]. TGF-β1 signals through different cytoplasmic proteins. We examined the effect of TGF-β1 on the expression of the cytoplasmic protein C184M using Western blot analysis. Cardiac myofibroblasts (P1) were plated in 100 mm dish and were grown to 70-80% confluency and starved for 24 hours and then stimulated with TGF-β1 (10 ng/ml) for 12, 24 and 48 hours. Total protein was then isolated and examined by Western blot analysis. As a positive control we used p-Smad2 which its expression is increased with TGF-β1 treatment. We found that C184M protein expression is not responsive to TGF-β1 treatment at different time points. β-tubulin was probed as a loading control. Results are shown for 24 and 48 hours treatment with TGF-β1 in figures 9 and 10, respectively. Result for 12 hours treatment was not shown.

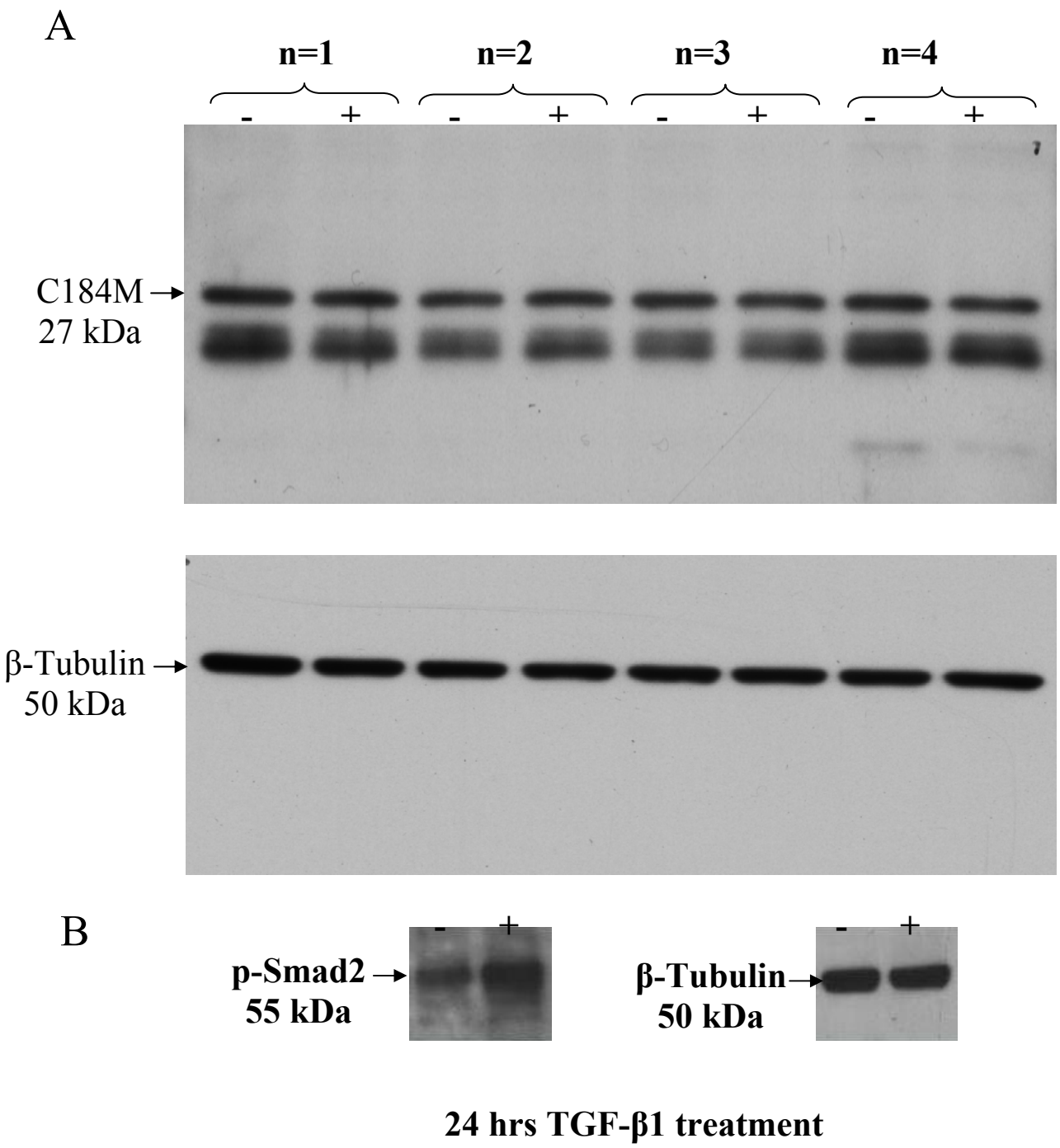

Figure 9. 24 hours TGF-β1 (10 ng/ml) treatment has no effect on C184M protein expression in primary cardiac myofibroblasts. P1 myofibroblasts were grown to 70-80% confluency, serum starved for 24 hours, and then either left unstimulated (-) or stimulated (+) with 10 ng/ml TGF-β1 for 24 hours. **Panel A:** representative Western blot showing levels of C184M (27 kDa) and β-Tubulin (50 kDa) as a loading control. Experiment was performed in quadruplicate (n=4). **Panel B:** representative Western blot showing levels of p-Smad2 (55 kDa) as a positive control for panel A and β-Tubulin (50 kda).

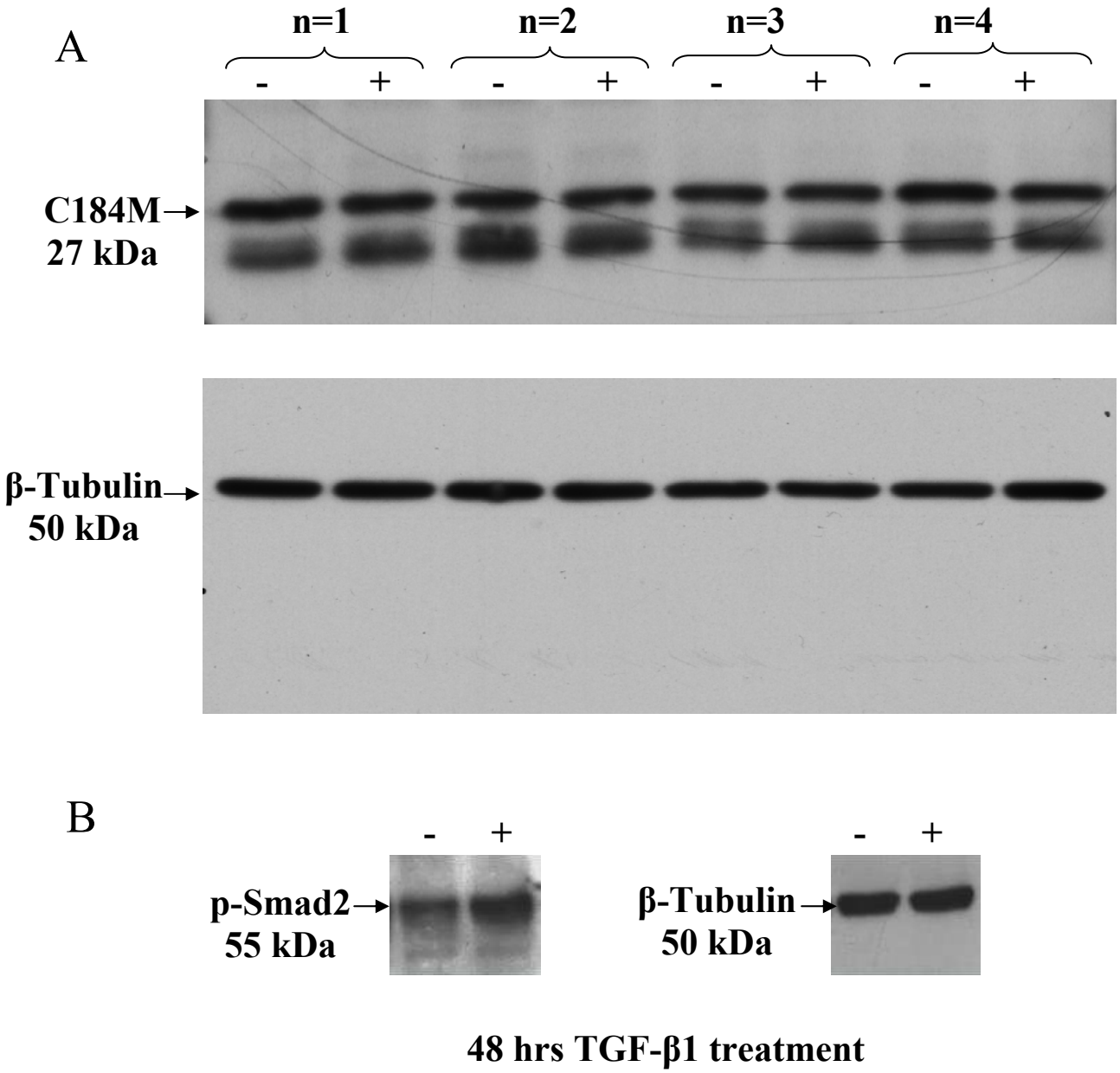

Figure 10. 48 hours TGF-β1 (10 ng/ml) treatment has no effect on C184M protein expression in primary cardiac myofibroblasts. P1 myofibroblasts were grown to 70-80% confluency, serum starved for 24 hours, and then either left unstimulated (-) or stimulated (+) with TGF-β1 for 48 hours. . **Panel A:** representative Western blot showing levels of C184M (27 kDa) and β-Tubulin (50 kDa) as a loading control. Experiment was performed in quadruplicate (n=4). **Panel B:** representative Western blot showing levels of p-Smad2 (55 kDa) as a positive control for panel A and β-Tubulin (50 kda).

4.0 Effect of Smad3 overexpression on the expression of C184M protein

Smad3 is a TGF-β signaling pathway downstream mediator, which modulates the transcription of target genes [197]. The effect of Smad3 on C184M expression at protein level was examined using Western blot analysis. P1 myofibroblasts were seeded in 100 mm dish and allowed to adhere overnight. Cells at 80% confluency were starved for 24 hours and then infected with Smad3 adenoviruses (10 MOI) for an additional 24 hours. Total protein was harvested and analyzed using Western blot. Smad3 overexpression did not influence expression of C184M protein. Results are shown in figure 11. Note that Smad3 level were increased in Smad3 adenovirus- infected cells.

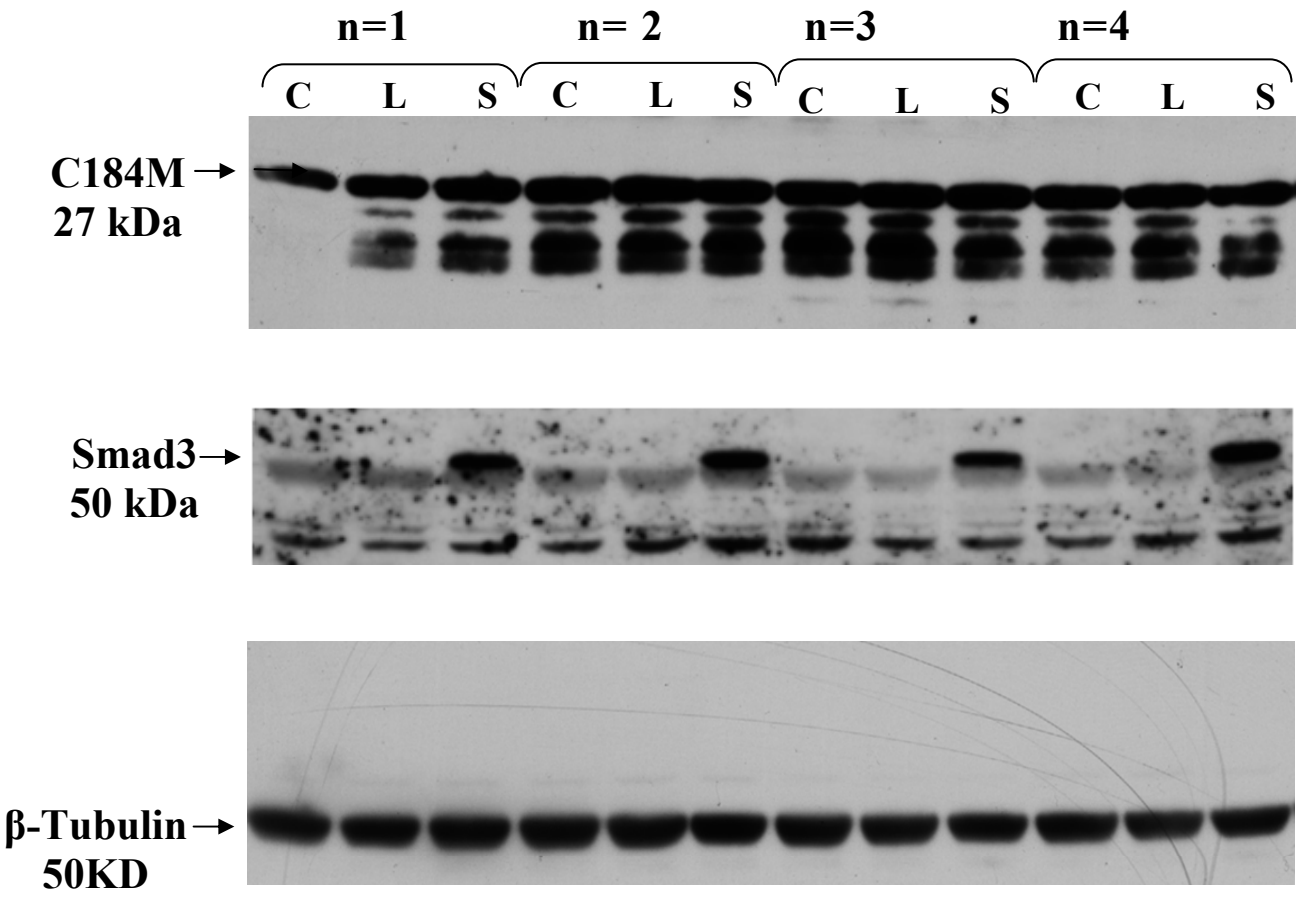

Figure 11. Smad3 overexpression does not influence expression of C184M protein. P1 myofibroblasts were grown to 70-80% confluency and serum starved for 24 hours. Cells were either left uninfected or infected with LacZ (100 MOI) or Smad 3 (10 MOI) for a further 24 hours. Control (C), LacZ (L), and Smad3 overexpressed (S).

5.0 Effect of C184M overexpression on Smad3 distribution in P1 cardiac myofibroblasts.

Primary fibroblasts (P0) were either left uninfected or infected at 20-40% confluency with the FLAG-C184M-EGFP or pMXIE-EGFP retroviruses (MOI 150 vp/cell) and allowed to grow to confluency before being passaged to obtain P1 cells. P1 cells were seeded onto the coverslips and used for immunofluorescence staining to examine the distribution of Smad3 in the presence of C184M overexpression. Our data showed a change from diffuse to punctate staining of Smad3 in the cytosol of C184M overexpressing cells (Figure 12). This finding may indicate a role for C184M in sequestering R-Smads such as Smad3 within the cell and this function may occur in parallel with its role as a docking protein for Ski –thus, a complex relationship between intracellular R-Smad signaling and C184M protein exists in primary cardiac myofibroblasts. Optimal MOI for FLAG-C184M-EGFP and pMXIE-EGFP retroviruses was confirmed using FACS machine. Right and left windows in Figure 13A indicate percentage of $EGFP^{+}$ (infected cells) and $EGFP^{-}$ (non-infected cells) expressing cells respectively. Figure 13B shows quantified data which had been obtained from FACS machines as shown in panel A.

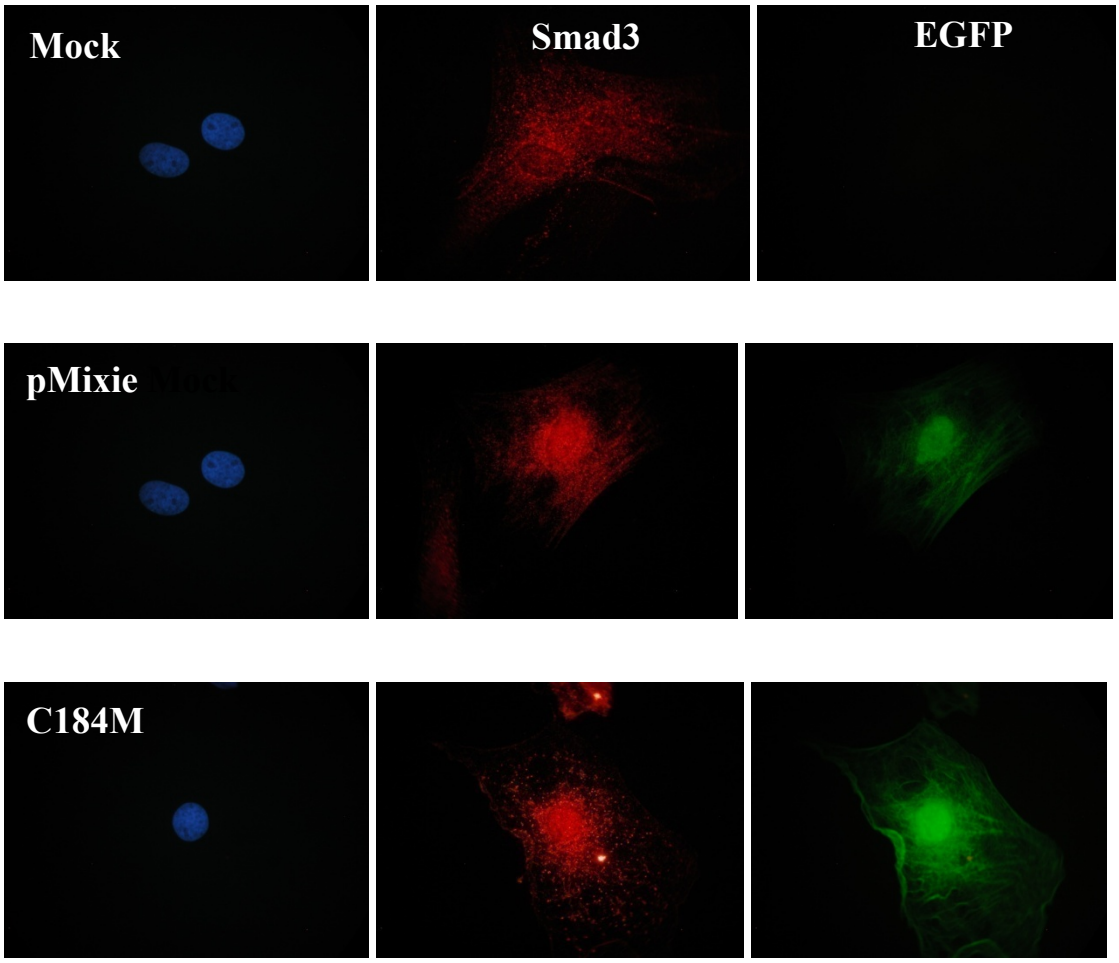

Figure 12. Smad3 distribution in P1 cardiac myofibroblasts is altered by C184M overexpression. P0 fibroblasts were either infected with retrovirus expressing FLAG-C184M and EGFP or left uninfected. P1 myofibroblasts were seeded onto coverslips and starved for 48 hours before immunofluorescence staining. Our results show altered staining of Smad3 in C184M overexpressing group.

A

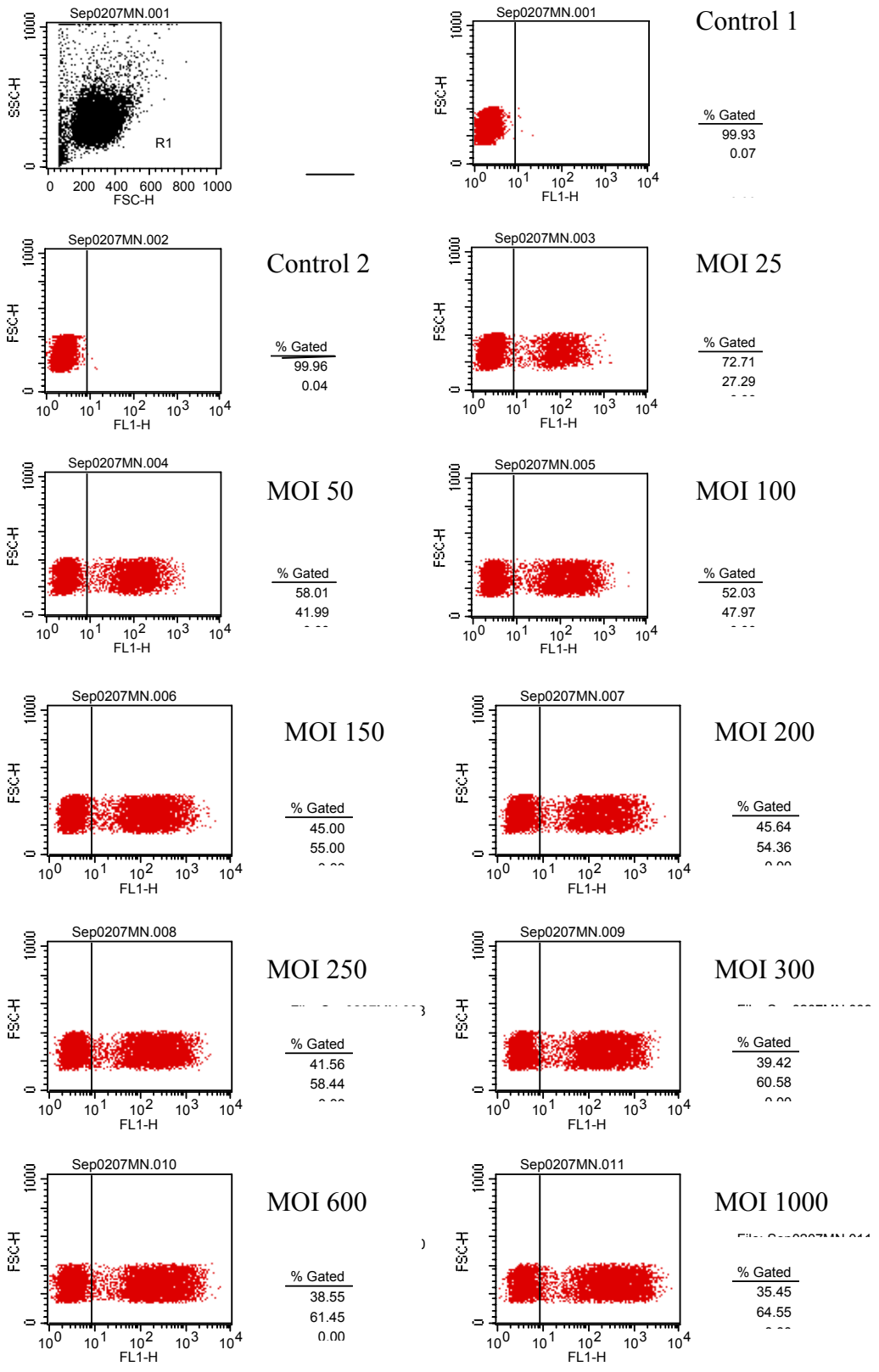

Figure 13. See legend next page

B

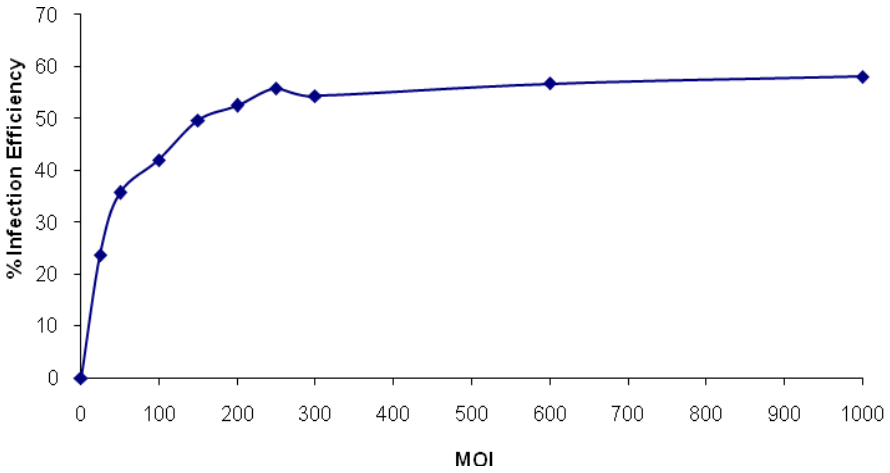

Figure 13. Optimization of MOI for FLAG-C184M-EGFP retroviruses in P0 cardiac fibroblasts. P0 fibroblasts (at 20-40%) confluency were subjected to C184M-EGFP retroviral infection using different MOIs (25, 50, 100, 150, 200, 250, 300, 600 and 1,000 vp/cell). Media was changed after 6 hours with fresh 10% FBS containing media. Cells were harvested to being analyzed using FACS machine at 100% confluency. EGFP was used as a markerof infection. MOI 150 was the most economized with highest infection efficiency. **Panel A:** P0 fibroblasts were analyzed using flow cytometry for $EGFP^{+}$ and $EGFP^{-}$ expression (Right and left windows respectively). **Panel B:** Graph of quantified data from groups shown in panel A. Each experimental group was performed in duplicate.

6.0 Effect of TGF-β1 stimulation on C184M localization in C184M overexpressing P1 cardiac myofibroblasts

P0 fibroblasts were either infected or left uninfected at 20-40% confluency with the FLAG-C184M-EGFP or pMXIE-EGFP retroviruses (MOI 150 vp/cell) and allowed to grow to confluency before being passaged to obtain P1 cells. P1 cells were seeded onto the coverslips and after 24 hours starvation, stimulated with TGF-β1(10 ng/ml) for an additional 24 hours. Cells were then subjected to immunofluorescence staining to examine the distribution of C184M in the presence and absence of TGF-β1 treatment. Our data show no changes in the localization of C184M in C184M overexpressing cells vs. controls (Figure 14).

A

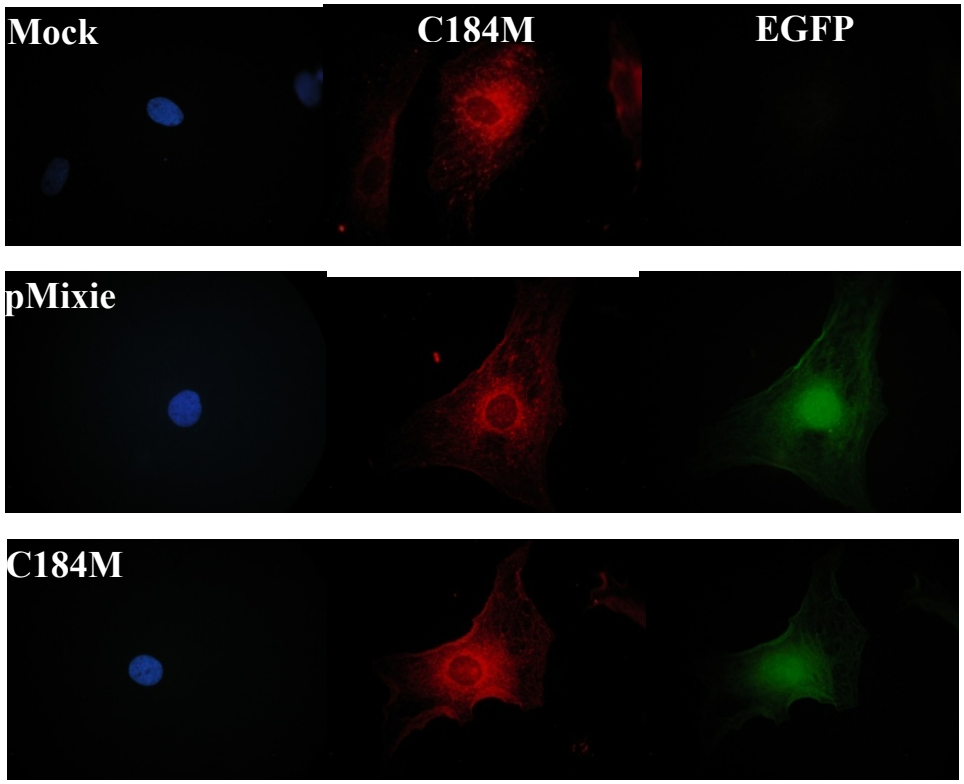
Mock
C184M
EGFP
pMixie
C184M

B

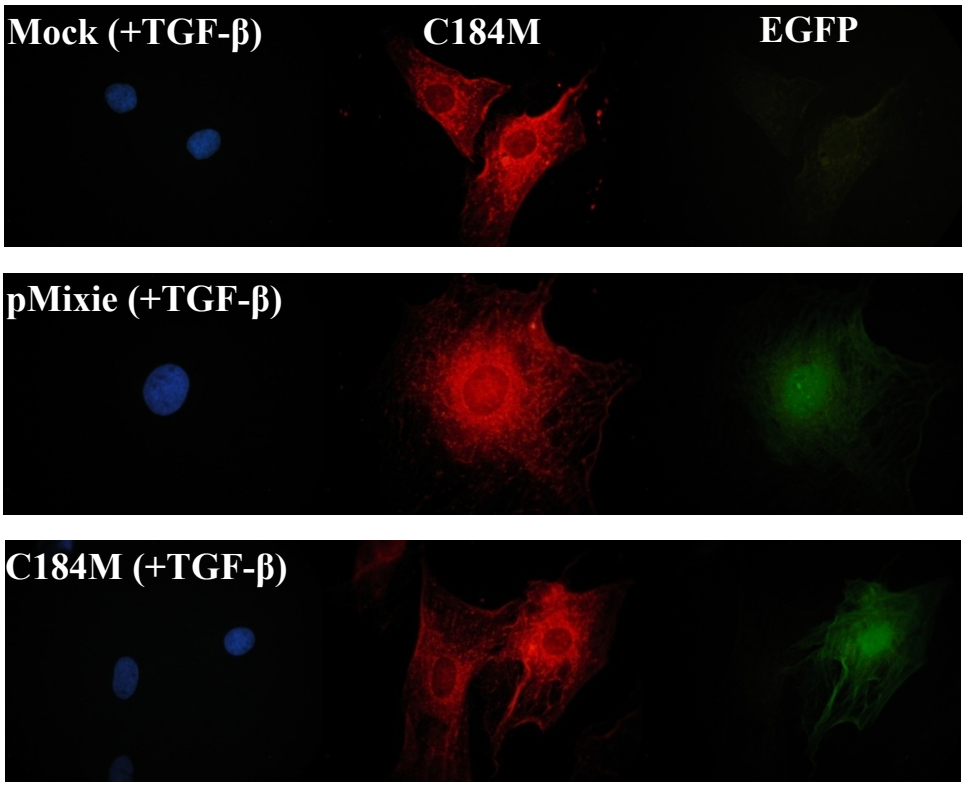
Mock (+TGF-β)
C184M
EGFP
pMixie (+TGF-β)
C184M (+TGF-β)

Figure 14. C184M distribution in P1 cardiac myofibroblasts is not altered by TGF-β1 treatment. P0 fibroblasts were infected with retrovirus expressing C184M and EGFP. Then P1 myofibroblasts were seeded onto coverslips, serum starved for 24 hours and stimulated with TGF-β1 for additional 24 hours. **Panel A:** shows C184M localization in the absence of TGF-β1 treatment. **Panel B:** shows C184M localization in the TGF-β1 treated cells.

7.0 Effect of overexpressed C184M on NIH 3T3 fibroblasts contractility in presence and absence of TGF-β1

The semi-anchored collagen type I gel deformation method was used to study the *in vitro* effects of C184M overexpression on NIH 3T3 fibroblasts contractility. Collagen gels were prepared and allowed to solidify overnight. Cells were plated on the surface of the gel and allowed to adhere and grow for 24 hours. Cells were then subjected to transfection with N-FLAG-pact-C184M plasmid using Lipofectamine^{TM} 2000 Reagent in antibiotic and serum free conditions. Application of TGF-β1 (10 ng/ml) was followed by detachment of the gel from the surrounding walls of the wells using a surgical blade, marking the initiation of the contraction phase. Wells were digitally photographed at 0 and 24 hours (Figure 15A). Gel surface area on a 2D digital image was quantified to assess the rate of contraction using Measure Gel custom software with IDL based analysis. Each experimental group was performed in quadruplicate. Figure 15B demonstrates that although contraction is augmented two fold in TGF-β1 (10 ng/ml) stimulated C184M overexpressing cells, C184M overexpression was associated with a 20% diminution of contraction compared to TGF-β1 control. Also we found no significant differences between C184M overexpressing cells and control group. Efficiency of transfection was confirmed using Western blot (Figure 16A). Our data show that transfected cells, express 5-fold more C184M protein compared with controls (Figure 16B). β-Tubulin was probed as a loading control.

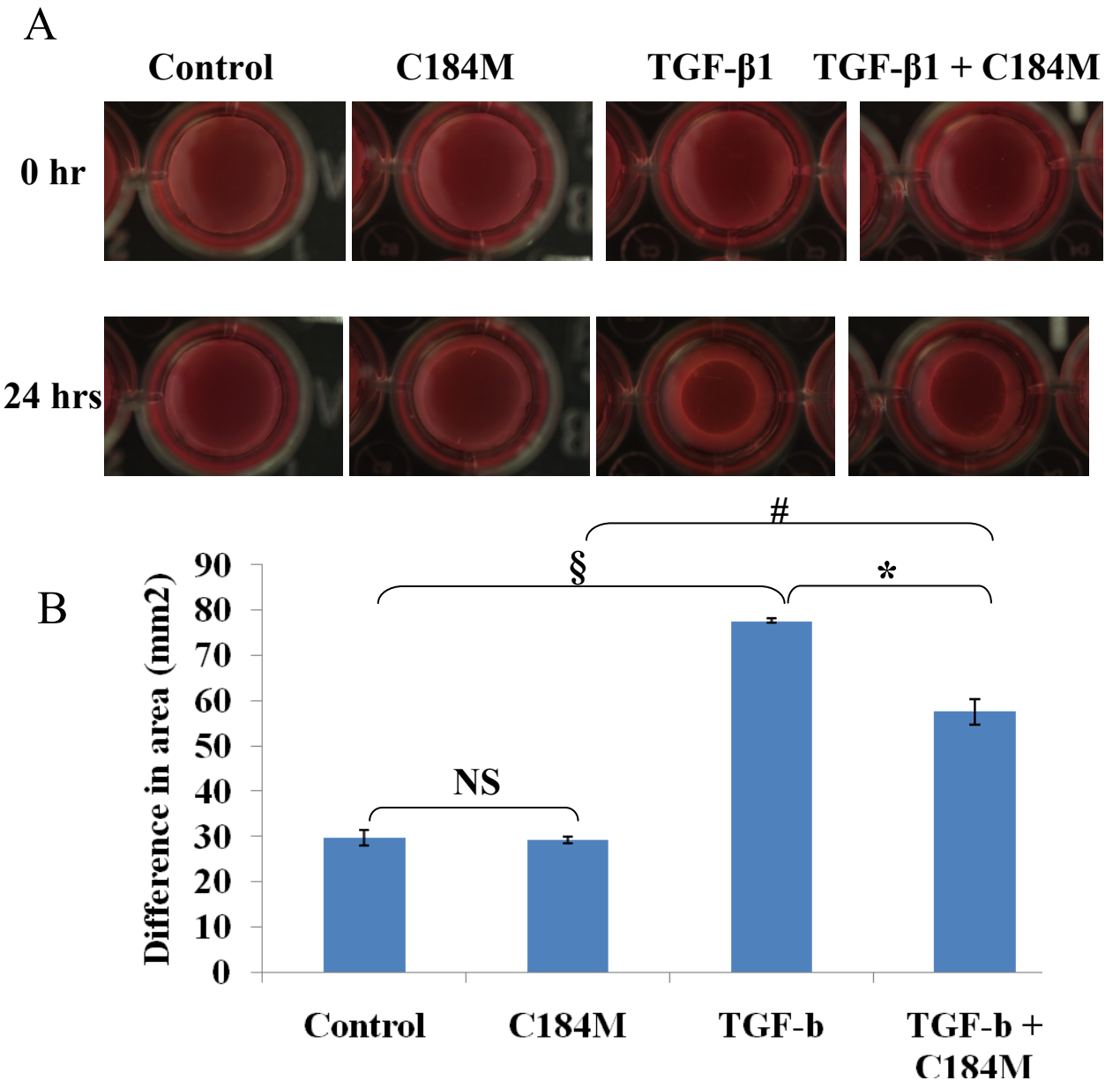

Figure 15. The role of C184M in modulation of NIH 3T3 fibroblasts contractility. Panel A: NIH 3T3 fibroblasts were loaded ($1x10^5$ cells/ml) onto preformed collagen type I gels. Following a 24 hours adherence and growth period, cells were transfected with pACTN-FLAG-C184M plasmid using Lipofectamine™ 2000 Reagent in antibiotic and serum-free conditions. Cells were then treated with TGF-β1 (10 ng/ml) for 24 hours. Digital images are shown of gel surfaces at 0 and 24 hours. **Panel B:** Gel surface area within the boundary of the contraction lines were measured with IDL based analysis and custom made Measure Gel software. The differences between gel areas of 0 and 24 h incubation periods were used to determine rate of cell contraction. Each experimental group was performed in quadruplicate (n=4). NS - Not significant. $^{\S}P < 0.001$ vs. control, $^{\#}P < 0.001$ vs. C184M, $^{*}P < 0.001$ vs. TGF-β; data are expressed as mean ± SE.

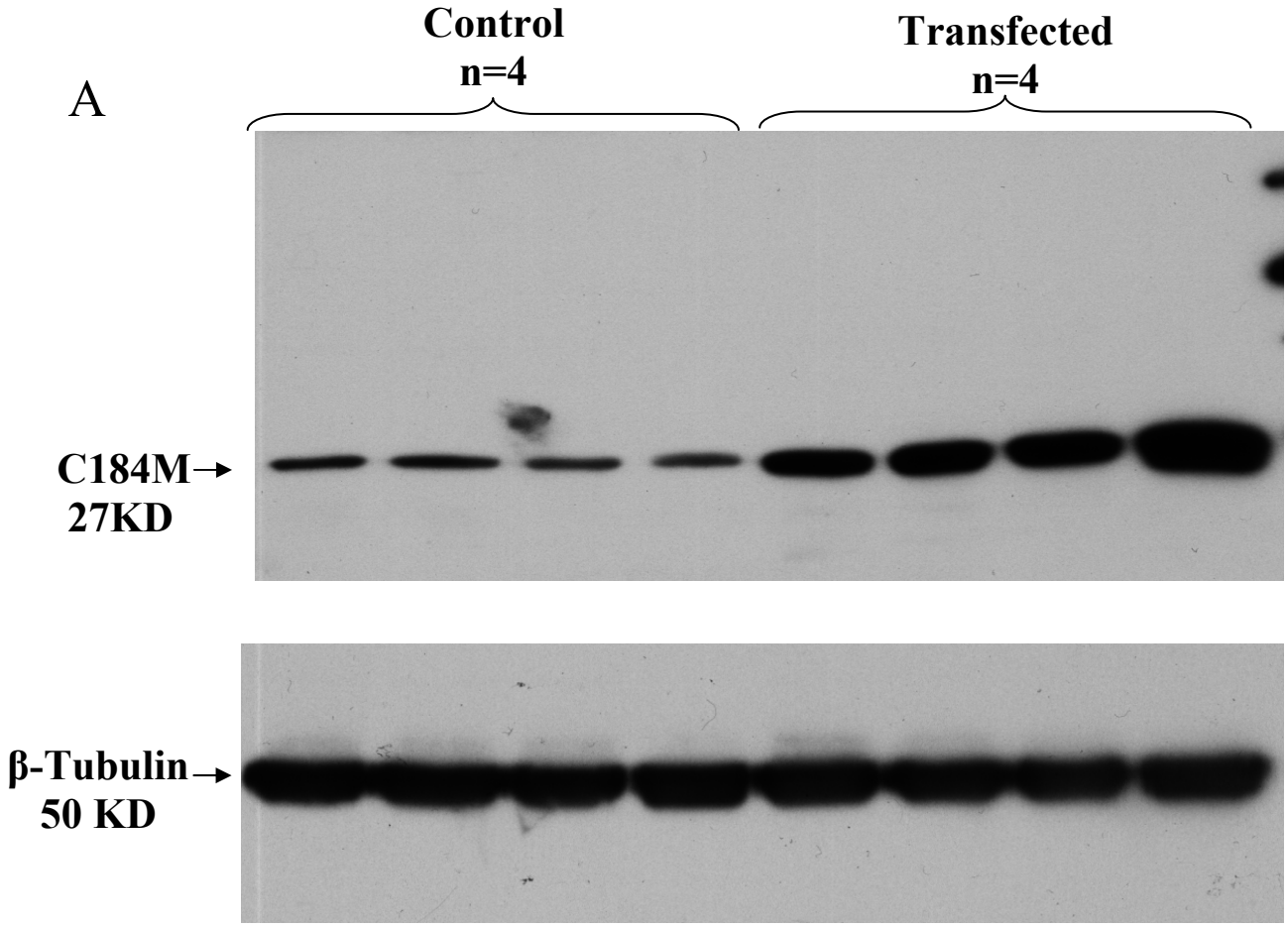
A
Control
n=4
Transfected
n=4
C184M→
27KD
β-Tubulin→
50 KD
B
Densitometry Units
2
1.8
1.6
1.4
1.2
1
0.8
0.6
0.4
0.2
0
Control
Transfected

Figure 16. Transfection efficiency in NIH 3T3 fibroblasts. NIH 3T3 fibroblasts were plated at $8.8x10^5$ cells/100 mm dish and allowed to adhere and grow overnight. The cells were subjected to transfection at 70-80% confluency with N-FLAG-pact-C184M using Lipofectamine™ 2000 Reagent in antibiotic and serum free condition. Total proteins were harvested 48 hours after transfection. **Panel A:** representative Western blot showing levels of C184M (27 kDa) and β-Tubulin (50 kDa). **Panel B:** Graph of quantified data from groups shown in panel A. Data quantified by densitometric scanning. All bands are normalized to β-Tubulin. Each experimental group was performed in quadruplicate (n=4).

8.0 Effect of overexpressed C184M on collagen secretion in presence and absence of TGF-β1

Collagen is an extracellular protein which is highly secreted in fibrosis. The TGF-β1 signaling pathway is involved in up-regulation of collagen synthesis and secretion. The role of C184M as a novel partner for co-repressor c-Ski in TGF-β1 signaling pathway is unclear. We examined the effects C184M overexpression on TGF-β1 induced collagen secretion in NIH 3T3 fibroblasts. The cells were plated in 100 mm dish and allowed to grow overnight. The cells were then subjected to transfection with N-FLAG-pact-C184M plasmid. After 24 hours starvation, groups were either stimulated with TGF-β1 or left unstimulated for additional 24 hours. The media and cells were collected and analyzed for collagen secretion using a PINP kit. Consistent with previous results from our lab, collagen secretion increased significantly in TGF-β1 stimulated cells compared to non-stimulated controls. However, C184M overexpression alone increased collagen secretion significantly relative to the non-stimulated control group. Interestingly, C184M overexpression in presence of TGF-β1 treatment significantly reduced the effect of TGF-β1 on collagen secretion suggesting inhibitory role of C184M in TGF-β1 signaling pathway (Figure 17).

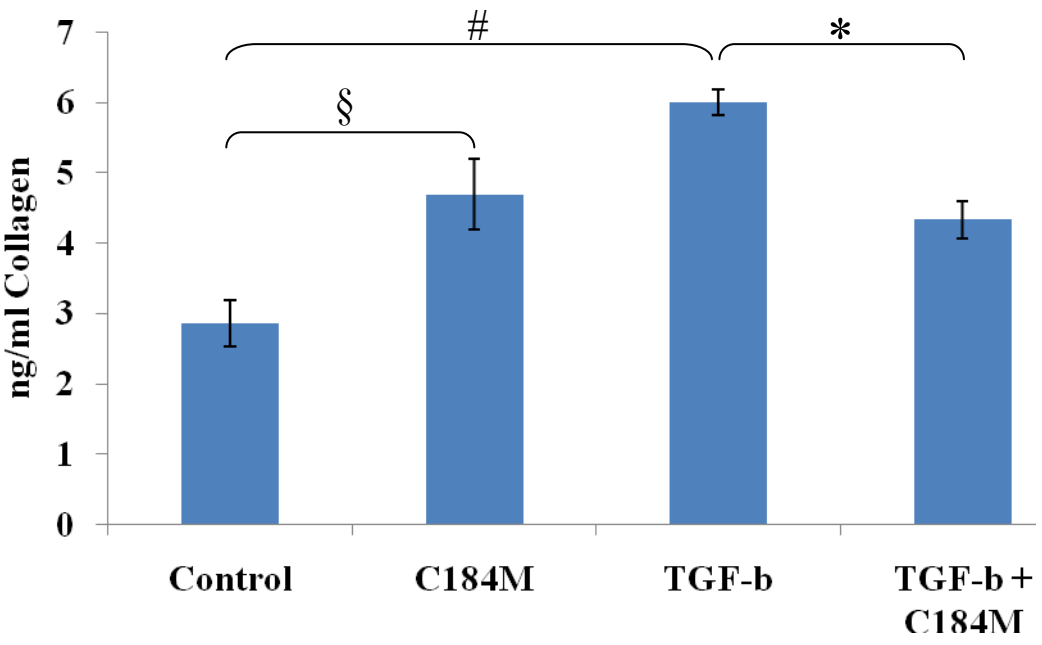

Figure 17. Collagen secretion in NIH 3T3 fibroblasts is altered by C184M overexpression in presence and absence of TGF-β1. Cells were grown to 70-80% confluency and subjected to transfection with N-FLAG-pact-C184M plasmid in antibiotic and serum-free conditions. After 24 hours of serum starvation, groups were either stimulated with TGF-β1 (10ng/ml) or left unstimulated for additional 24 hours. Harvested media and cells were analyzed for collagen secretion using PINP kit. Graph shows the quantified data from spectrophotometer results. $^{\S}P = 0.007$ vs. control, $^{\#}P < 0.001$ vs. control, $^{*}P = 0.012$ vs. TGF-β1; data are expressed as mean ± SE. Each experimental group was performed in quadruplicate (n=4).

VI Discussion

In this study we examined Ski-interacting protein C184M mRNA and protein expression in P0 primary cardiac fibroblasts, as well as P1 and P2 cardiac myofibroblasts and NIH 3T3 fibroblasts. The C184M gene was originally identified in developing mouse brain [198] and has been shown to interact with Ski via its leucine-rich region [199]. Ski is a nuclear protein, but it is known that C184M associates with Ski, and functions to sequester Ski in the cytosol [200]. Consistent with this finding, Ski has been found to be localized in the cytosol of hepatocytes that express high level of C184M protein [201]. As Ski is involved in TGF-β signaling and may suppress the expression of TGF-β responsive genes[202], C184M may also play a role in TGF-β modulated cellular function. TGF-β is a pleuripotent cytokine which is highly expressed in the infarct scar following myocardial infarction [13, 203]. Although TGF-β induces the expression of different genes including collagens type I and III [107], we have demonstrated that C184M expression itself is not responsive to TGF-β1 treatment (10 ng/ml for 12, 24, and 48 hours) and thus may be a stably expressed regulatory protein or regulated by something else.

1.0 Relationship between C184M and Smad3 in ventricular myofibroblasts.

Immunofluorescence staining of C184M in myofibroblasts revealed the cytosolic localization of this protein, consistent with its localization in CV-1 cells and hepatocytes [204]. We also showed that TGF-β1 itself does not influence C184M localization in myofibroblasts. R-Smads, including Smad2 and Smad3, are major mediators in TGF-β signaling pathway post-MI in cardiac ventricular myofibroblasts. Following the binding of TGF-β ligand to TβRII and activation of TβRI, R-Smads undergo phosphorylation and initiate TGF-β transduction [205]. We found that C184M expression is not responsive to

Smad3 overexpression in ventricular myofibroblasts. Despite this lack of responsiveness of C184M expression to Smad3 overexpression, immunofluorescence staining of Smad3 in C184M overexpressing myofibroblasts indicated altered distribution of Smad3. The distribution of Smad3 was altered from diffuse pattern to a punctate staining pattern. This finding may indicate a role for C184M in sequestering R-Smads such as Smad3 within the cell and this function may occur in parallel with its role as a docking protein for Ski – thus, it may be a sign of a complex relationship between intracellular R-Smad signaling and C184M in primary cardiac myofibroblasts.

2.0 C184M expression and cardiac ventricular myofibroblasts function.

The main findings of the present study address the secretion of collagen type I in C184M overexpressing NIH3T3 fibroblasts and the effect of C184M overexpression on their contractility. Expression of TGF-β1 is markedly induced in the infarcted myocardium and plays a pivotal role in initiation and development of fibrosis [206-209] by induction of different genes expression including, collagen [107, 210], and fibronectin [211]. We measured the collagen production in NIH 3T3 fibroblasts via estimation of secretion of N-terminal globular ends of type I fibrillar collagen, and found that overexpression of C184M alone upregulates collagen production in the unstimulated basal state. Paradoxically, C184M overexpression is associated with suppressed collagen secretion in TGF-β1 stimulated NIH 3T3 fibroblasts. It has been shown that the association of C184M and Ski results in accumulation of Ski in the cytosol of CV-1 cells [212]. Thus we speculated that the elevation of collagen production in NIH-3T3 fibroblasts by C184M in the basal state may be the result of docking of Ski and its net sequestration in the cytosol by C184M. As Ski is a transcriptional co-repressor and inhibits expression of different

genes, cytosolic sequestrations of it may depress its effects on gene expression and as result may contribute to the relaxing of Ski's inhibitory effects and thus allow basal collagen production to increase. However, C184M suppresses TGF-β1 effects on collagen secretion in NIH 3T3 fibroblasts when they are stimulated with TGF-β1. To explain this, we suggest that Ski may be activated to bind Smads 2, 3 and 4 and thereby repress TGF-β1 transduction as has been observed in other studies [213-215]. In preinvasive melanoma cells, Ski localizes mainly to the cytosol, and these cells demonstrate diminished nuclear translocation of R-Smad3[216]. Grimm *et al* [217] documented that nuclear exclusion of R-Smad2 is a mechanism leading to loss of mesodermal competence during the early development of *Xenopus laevis*. Thus, suppression of collagen secretion in TGF-β1 stimulated cells by overexpressed C184M may be explained by the retention of R-Smads in the cytosol by the C184M-Ski complex, as it has been shown in CV-1 cells by Kokura *et al* [218]. Thus, it could be argued that sequestered R-Smads in the cytosol may be unable to translocate into the nucleus in the face of C184M overexpression, and as a result cannot induce expression of collagen gene. Additionally, we demonstrated, for the first time, that C184M overexpression is associated with significant attenuation of contractility in NIH 3T3 fibroblasts in the presence of TGF-β1. We employed a modified anchored assay wherein the gel edge is released from the plate at time zero in a 24 hours treatment regimen. NIH 3T3 fibroblasts are seeded on the surface of the matrix, and the reduction of matrices' surface is measured. Thus, collagen gel deformation reflects cellular contractility as well as remodeling of the matrices and is an *in vitro* model of wound contraction. While the precise mode of C184M-mediated inhibition of NIH 3T3 fibroblasts contraction is unknown, however as in collagen secretion inhibition (above), it

may operate via cytosolic retention of R-Smad proteins. This then mediates negative regulation of TGF-β1 signaling in NIH 3T3 fibroblasts resulting in decreased contraction.

VII Conclusions

1. We have identified that C184M is relatively highly expressed in P0 primary cardiac fibroblasts, P1 and P2 cardiac myofibroblasts and in the NIH 3T3 fibroblast cell line.
2. C184M expression is not responsive to TGF-β1 treatment at various times (10ng/ml 12, 24 and 48 hours) in primary myofibroblasts.
3. Smad3 overexpression has no impact on C184M expression in myofibroblasts. However, diffuse cytosolic distribution becomes localized to points (punctuate staining) in C184M overexpressing myofibroblasts.
4. Overexpression of C184M was characterized with a biphasic effect on collagen type I N-terminal peptide secretion in NIH 3T3 fibroblasts. Specifically in starved unstimulated fibroblasts it elevates collagen secretion while in TGF-β1 stimulated cells it suppresses TGF-β1 induced collagen secretion.
5. C184M overexpression significantly attenuates TGF-β-mediated contractility in TGF-β1-treated NIH 3T3 fibroblasts.

VIII Future Directions

We have documented the expression of C184M in primary cardiac fibroblasts and myofibroblasts and in NIH 3T3 fibroblasts. Contractility and collagen secretion data demonstrated that C184M negatively regulates TGF-β1-mediated stimulation of fibroblast functions. It would be worthwhile to knock down C184M expression using RNAi technology (shRNA) and explore its effects on the contractility and collagen secretion in these cells. To further confirm the effects of C184M on contractility and collagen secretion we would also rescue C184M knock down expression using overexpression methods and then determine myofibroblasts contractility and collagen secretion vs controls.

As C184M is involved in TGF-β signaling and its own expression is not responsive to TGF-β stimulation, it would be worthwhile to study C184M structure and explore the possibility of potential sites that undergo post-translational modifications including Ser/Thr phosphorylation following TGF-β1 (or other cytokines eg, AII, CT-1) treatment which may impinge upon C184M expression or function.

We have shown that Ski is expressed in both cardiac fibroblasts and myofibroblasts. Previous studies has highlighted the fact that Ski plays a role in the development of muscle[219] and the Ski-null mice suffer from decreased skeletal muscle mass[220]. In quail embryos Ski causes transformation and muscle differentiation of fibroblastic cells. Fibroblasts phenotypically convert to myofibroblasts by expressing α-SMA [5, 52]and SMemb [221]. As Ski is involves in muscle development, it may induce the phenotypic shift to myofibroblasts; thus C184M as a Ski binding partner may influence induction. It would be a valuable exercise to follow up on this posibility.

We identified altered distribution of Smad3 in C184M overdriven myofibroblasts. Immunofluorescence staining for both C184M and Smad3 would clarify if there is any co-localization of these two proteins in these experimental conditions. Finally, C184M increases the expression of Ski in CV-1, 293T and Mv1Lu cells [222]. It would be interesting to observe whether, C184M has the same effect and elevates the amount of Ski in our experimental systems.

IX Literature cited

Reference List

1. Karalis DG. Intensive lowering of low-density lipoprotein cholesterol levels for primary prevention of coronary artery disease. Mayo Clin Proc 2009 Apr; 84(4): 345-52.

2. Jennings RB, Murry CE, Steenbergen C, Jr., Reimer KA. Development of cell injury in sustained acute ischemia
1. Circulation 1990 Sep; 82(3 Suppl): II2-12.

3. Pfeffer MA, Braunwald E. Ventricular remodeling after myocardial infarction. Experimental observations and clinical implications. Circulation 1990; 81(4): 1161-72.

4. Opie LH, Commerford PJ, Gersh BJ, Pfeffer MA. Controversies in ventricular remodelling
1. Lancet 2006 Jan 28; 367(9507): 356-67.

5. Darby I, Skalli O, Gabbiani G. Alpha-smooth muscle actin is transiently expressed by myofibroblasts during experimental wound healing. Lab Invest 1990; 63(1): 21-9.

6. Wang J, Chen H, Seth A, McCulloch CA. Mechanical force regulation of myofibroblast differentiation in cardiac fibroblasts. Am J Physiol Heart Circ Physiol 2003 Nov; 285(5): H1871-H1881.

7. Cleutjens JP, Verluyten MJ, Smits JF, Daemen MJ. Collagen remodeling after myocardial infarction in the rat heart. Am J Pathol 1995; 147(2): 325-38.

8. Tomasek JJ, Gabbiani G, Hinz B, Chaponnier C, Brown RA. Myofibroblasts and mechano-regulation of connective tissue remodelling. Nat Rev Mol Cell Biol 2002 May; 3(5): 349-63.

9. Weber KT, Sun Y, Cleutjens JP. Structural remodeling of the infarcted rat heart. Exs 1996; 76: 489-99.

10. Squires CE, Escobar GP, Payne JF, Leonardi RA, Goshorn DK, Sheats NJ, et al. Altered fibroblast function following myocardial infarction. J Mol Cell Cardiol 2005 Oct; 39(4): 699-707.

11. Tomasek JJ, Gabbiani G, Hinz B, Chaponnier C, Brown RA. Myofibroblasts and mechano-regulation of connective tissue remodelling. Nat Rev Mol Cell Biol 2002 May; 3(5): 349-63.

12. Jugdutt BI. Limiting fibrosis after myocardial infarction. N Engl J Med 2009 Apr 9; 360(15): 1567-9.

13. Thompson NL, Bazoberry F, Speir EH, Casscells W, Ferrans VJ, Flanders KC, et al. Transforming growth factor beta-1 in acute myocardial infarction in rats. Growth Factors 1988; 1(1): 91-9.

14. Ikeuchi M, Tsutsui H, Shiomi T, Matsusaka H, Matsushima S, Wen J, et al. Inhibition of TGF-beta signaling exacerbates early cardiac dysfunction but prevents late remodeling after infarction. Cardiovasc Res 2004 Dec 1; 64(3): 526-35.

15. Okada H, Kawaguchi H, Kudo T, Sawa H, Okamoto H, Watanabe S, et al. Alteration of extracellular matrix in dilated cardiomyopathic hamster heart. Mol Cell Biochem 1996; 156(1): 9-15.

16. Okada H, Takemura G, Kosai K, Li Y, Takahashi T, Esaki M, et al. Postinfarction gene therapy against transforming growth factor-beta signal modulates infarct tissue dynamics and attenuates left ventricular remodeling and heart failure. Circulation 2005 May 17; 111(19): 2430-7.

17. Zhao XH, Laschinger C, Arora P, Szaszi K, Kapus A, McCulloch CA. Force activates smooth muscle alpha-actin promoter activity through the Rho signaling pathway. J Cell Sci 2007 May 15; 120(Pt 10): 1801-9.

18. Li P, Wang D, Lucas J, Oparil S, Xing D, Cao X, et al. Atrial natriuretic peptide inhibits transforming growth factor beta-induced Smad signaling and myofibroblast transformation in mouse cardiac fibroblasts. Circ Res 2008 Feb 1; 102(2): 185-92.

19. Malmstrom J, Lindberg H, Lindberg C, Bratt C, Wieslander E, Delander EL, et al. Transforming growth factor-beta 1 specifically induce proteins involved in the myofibroblast contractile apparatus. Mol Cell Proteomics 2004 May; 3(5): 466-77.

20. Verrecchia F, Mauviel A. Transforming growth factor-beta and fibrosis. World J Gastroenterol 2007 Jun 14; 13(22): 3056-62.

21. Luo K, Stroschein SL, Wang W, Chen D, Martens E, Zhou S, et al. The Ski oncoprotein interacts with the Smad proteins to repress TGFbeta signaling. Genes Dev 1999 Sep 1; 13(17): 2196-206.

22. Akiyoshi S, Inoue H, Hanai J, Kusanagi K, Nemoto N, Miyazono K, et al. c-Ski acts as a transcriptional co-repressor in transforming growth factor-beta signaling through interaction with smads. J Biol Chem 1999 Dec 3; 274(49): 35269-77.

23. Sun Y, Liu X, Eaton EN, Lane WS, Lodish HF, Weinberg RA. Interaction of the Ski oncoprotein with Smad3 regulates TGF-beta signaling. Mol Cell 1999 Oct; 4(4): 499-509.

24. Xu W, Angelis K, Danielpour D, Haddad MM, Bischof O, Campisi J, et al. Ski acts as a co-repressor with Smad2 and Smad3 to regulate the response to type beta transforming growth factor. Proc Natl Acad Sci U S A 2000 May 23; 97(11): 5924-9.

25. Arndt S, Poser I, Moser M, Bosserhoff AK. Fussel-15, a novel Ski/Sno homolog protein, antagonizes BMP signaling. Mol Cell Neurosci 2007 Apr; 34(4): 603-11.

26. Arndt S, Poser I, Schubert T, Moser M, Bosserhoff AK. Cloning and functional characterization of a new Ski homolog, Fussel-18, specifically expressed in neuronal tissues. Lab Invest 2005 Nov; 85(11): 1330-41.

27. Liu X, Zhang E, Li P, Liu J, Zhou P, Gu DY, et al. Expression and possible mechanism of c-ski, a novel tissue repair-related gene during normal and radiation-impaired wound healing. Wound Repair Regen 2006 Mar; 14(2): 162-71.

28. Wu JW, Krawitz AR, Chai J, Li W, Zhang F, Luo K, et al. Structural mechanism of Smad4 recognition by the nuclear oncoprotein Ski: insights on Ski-mediated repression of TGF-beta signaling. Cell 2002 Nov 1; 111(3): 357-67.

29. Harada J, Kokura K, Kanei-Ishii C, Nomura T, Khan MM, Kim Y, et al. Requirement of the co-repressor homeodomain-interacting protein kinase 2 for ski-mediated inhibition of bone morphogenetic protein-induced transcriptional activation
1. J Biol Chem 2003 Oct 3; 278(40): 38998-9005.

30. Ayer DE, Lawrence QA, Eisenman RN. Mad-Max transcriptional repression is mediated by ternary complex formation with mammalian homologs of yeast repressor Sin3
1. Cell 1995 Mar 10; 80(5): 767-76.

31. Akiyoshi S, Inoue H, Hanai J, Kusanagi K, Nemoto N, Miyazono K, et al. c-Ski acts as a transcriptional co-repressor in transforming growth factor-beta signaling through interaction with smads. J Biol Chem 1999 Dec 3; 274(49): 35269-77.

32. Wu JW, Krawitz AR, Chai J, Li W, Zhang F, Luo K, et al. Structural mechanism of Smad4 recognition by the nuclear oncoprotein Ski: insights on Ski-mediated repression of TGF-beta signaling. Cell 2002 Nov 1; 111(3): 357-67.

33. Kokura K, Kim H, Shinagawa T, Khan MM, Nomura T, Ishii S. The Ski-binding protein C184M negatively regulates tumor growth factor-beta signaling by sequestering the Smad proteins in the cytoplasm. J Biol Chem 2003 May 30; 278(22): 20133-9.

34. Kokura K, Kim H, Shinagawa T, Khan MM, Nomura T, Ishii S. The Ski-binding protein C184M negatively regulates tumor growth factor-beta signaling by sequestering the Smad proteins in the cytoplasm. J Biol Chem 2003 May 30; 278(22): 20133-9.

35. Karalis DG. Intensive lowering of low-density lipoprotein cholesterol levels for primary prevention of coronary artery disease. Mayo Clin Proc 2009 Apr; 84(4): 345-52.

36. Jennings RB, Murry CE, Steenbergen C, Jr., Reimer KA. Development of cell injury in sustained acute ischemia
1. Circulation 1990 Sep; 82(3 Suppl): II2-12.

37. Jennings RB, Reimer KA. The cell biology of acute myocardial ischemia. Annu Rev Med 1991; 42: 225-46.

38. Opie LH, Commerford PJ, Gersh BJ, Pfeffer MA. Controversies in ventricular remodelling
1. Lancet 2006 Jan 28; 367(9507): 356-67.

39. Frangogiannis NG. The mechanistic basis of infarct healing
19. Antioxid Redox Signal 2006 Nov; 8(11-12): 1907-39.

40. Birdsall HH, Green DM, Trial J, Youker KA, Burns AR, MacKay CR, et al. Complement C5a, TGF-beta 1, and MCP-1, in sequence, induce migration of monocytes into ischemic canine myocardium within the first one to five hours after reperfusion. Circulation 1997 Feb 4; 95(3): 684-92.

41. Frangogiannis NG. Chemokines in ischemia and reperfusion. Thromb Haemost 2007 May; 97(5): 738-47.

42. Frangogiannis NG, Smith CW, Entman ML. The inflammatory response in myocardial infarction. Cardiovasc Res 2002 Jan; 53(1): 31-47.

43. Cleutjens JP, Blankesteijn WM, Daemen MJ, Smits JF. The infarcted myocardium: simply dead tissue, or a lively target for therapeutic interventions. Cardiovasc Res 1999; 44(2): 232-41.

44. Lambert JM, Lopez EF, Lindsey ML. Macrophage roles following myocardial infarction. Int J Cardiol 2008 Nov 12; 130(2): 147-58.

45. Ren G, Dewald O, Frangogiannis NG. Inflammatory mechanisms in myocardial infarction. Curr Drug Targets Inflamm Allergy 2003; 2(3): 242-56.

46. Singer AJ, Clark RA. Cutaneous wound healing. N Engl J Med 1999 Sep 2; 341(10): 738-46.

47. Virag JI, Murry CE. Myofibroblast and endothelial cell proliferation during murine myocardial infarct repair. Am J Pathol 2003 Dec; 163(6): 2433-40.

48. Lambert JM, Lopez EF, Lindsey ML. Macrophage roles following myocardial infarction. Int J Cardiol 2008 Nov 12; 130(2): 147-58.

49. Gabbiani G. The cellular derivation and the life span of the myofibroblast. Pathol Res Pract 1996; 192(7): 708-11.

50. Gabbiani G, Le LM, Bailey AJ, Bazin S, Delaunay A. Collagen and myofibroblasts of granulation tissue. A chemical, ultrastructural and immunologic study. Virchows Arch B Cell Pathol 1976 Aug 11; 21(2): 133-45.

51. Frangogiannis NG. The mechanistic basis of infarct healing
19. Antioxid Redox Signal 2006 Nov; 8(11-12): 1907-39.

52. Willems IE, Havenith MG, De Mey JG, Daemen MJ. The alpha-smooth muscle actin-positive cells in healing human myocardial scars. Am J Pathol 1994; 145(4): 868-75.

53. van Amerongen MJ, Bou-Gharios G, Popa E, van AJ, Petersen AH, van Dam GM, et al. Bone marrow-derived myofibroblasts contribute functionally to scar formation after myocardial infarction
2. J Pathol 2008 Feb; 214(3): 377-86.

54. Sappino AP, Schurch W, Gabbiani G. Differentiation repertoire of fibroblastic cells: expression of cytoskeletal proteins as marker of phenotypic modulations. Lab Invest 1990; 63(2): 144-61.

55. Frangogiannis NG, Michael LH, Entman ML. Myofibroblasts in reperfused myocardial infarcts express the embryonic form of smooth muscle myosin heavy chain (SMemb). Cardiovasc Res 2000 Oct; 48(1): 89-100.

56. Arora PD, McCulloch CA. Dependence of collagen remodelling on alpha-smooth muscle actin expression by fibroblasts. J Cell Physiol 1994 Apr; 159(1): 161-75.

57. Gabbiani G, Hirschel BJ, Ryan GB, Statkov PR, Majno G. Granulation tissue as a contractile organ. A study of structure and function. J Exp Med 1972 Apr 1; 135(4): 719-34.

58. Hinz B, Celetta G, Tomasek JJ, Gabbiani G, Chaponnier C. Alpha-smooth muscle actin expression upregulates fibroblast contractile activity. Mol Biol Cell 2001 Sep; 12(9): 2730-41.

59. Vracko R, Thorning D. Contractile cells in rat myocardial scar tissue. Lab Invest 1991; 65(2): 214-27.

60. Campbell SE, Katwa LC. Angiotensin II stimulated expression of transforming growth factor- beta1 in cardiac fibroblasts and myofibroblasts. J Mol Cell Cardiol 1997 Jul; 29(7): 1947-58.

61. Katwa LC. Cardiac myofibroblasts isolated from the site of myocardial infarction express endothelin de novo. Am J Physiol Heart Circ Physiol 2003 Sep; 285(3): H1132-H1139.

62. Massague J, Gomis RR. The logic of TGFbeta signaling. FEBS Lett 2006 May 22; 580(12): 2811-20.

63. Verrecchia F, Mauviel A. Transforming growth factor-beta and fibrosis. World J Gastroenterol 2007 Jun 14; 13(22): 3056-62.

64. Xiao H, Zhang YY. Understanding the role of transforming growth factor-beta signalling in the heart: overview of studies using genetic mouse models. Clin Exp Pharmacol Physiol 2008 Mar; 35(3): 335-41.

65. Xiao H, Zhang YY. Understanding the role of transforming growth factor-beta signalling in the heart: overview of studies using genetic mouse models. Clin Exp Pharmacol Physiol 2008 Mar; 35(3): 335-41.

66. Verrecchia F, Mauviel A. Transforming growth factor-beta and fibrosis. World J Gastroenterol 2007 Jun 14; 13(22): 3056-62.

67. Bujak M, Frangogiannis NG. The role of TGF-beta signaling in myocardial infarction and cardiac remodeling. Cardiovasc Res 2007 May 1; 74(2): 184-95.

68. Letterio JJ, Roberts AB. Regulation of immune responses by TGF-beta. Annu Rev Immunol 1998; 16: 137-61.

69. Frangogiannis NG. The immune system and cardiac repair
3. Pharmacol Res 2008 Aug; 58(2): 88-111.

70. Dickson MC, Martin JS, Cousins FM, Kulkarni AB, Karlsson S, Akhurst RJ. Defective haematopoiesis and vasculogenesis in transforming growth factor-beta 1 knock out mice. Development 1995 Jun; 121(6): 1845-54.

71. Kulkarni AB, Huh CG, Becker D, Geiser A, Lyght M, Flanders KC, et al. Transforming growth factor beta 1 null mutation in mice causes excessive inflammatory response and early death. Proc Natl Acad Sci U S A 1993 Jan 15; 90(2): 770-4.

72. Sanford LP, Ormsby I, Gittenberger-de Groot AC, Sariola H, Friedman R, Boivin GP, et al. TGFbeta2 knockout mice have multiple developmental defects that are

non-overlapping with other TGFbeta knockout phenotypes. Development 1997 Jul; 124(13): 2659-70.

73. Proetzel G, Pawlowski SA, Wiles MV, Yin M, Boivin GP, Howles PN, et al. Transforming growth factor-beta 3 is required for secondary palate fusion. Nat Genet 1995 Dec; 11(4): 409-14.

74. Ikeuchi M, Tsutsui H, Shiomi T, Matsusaka H, Matsushima S, Wen J, et al. Inhibition of TGF-beta signaling exacerbates early cardiac dysfunction but prevents late remodeling after infarction. Cardiovasc Res 2004 Dec 1; 64(3): 526-35.

75. Okada H, Takemura G, Kosai K, Li Y, Takahashi T, Esaki M, et al. Postinfarction gene therapy against transforming growth factor-beta signal modulates infarct tissue dynamics and attenuates left ventricular remodeling and heart failure. Circulation 2005 May 17; 111(19): 2430-7.

76. Deten A, Holzl A, Leicht M, Barth W, Zimmer HG. Changes in extracellular matrix and in transforming growth factor beta isoforms after coronary artery ligation in rats. J Mol Cell Cardiol 2001 Jun; 33(6): 1191-207.

77. Dewald O, Ren G, Duerr GD, Zoerlein M, Klemm C, Gersch C, et al. Of mice and dogs: species-specific differences in the inflammatory response following myocardial infarction. Am J Pathol 2004 Feb; 164(2): 665-77.

78. Gawaz M, Langer H, May AE. Platelets in inflammation and atherogenesis. J Clin Invest 2005 Dec; 115(12): 3378-84.

79. Dean RG, Balding LC, Candido R, Burns WC, Cao Z, Twigg SM, et al. Connective tissue growth factor and cardiac fibrosis after myocardial infarction. J Histochem Cytochem 2005 Oct; 53(10): 1245-56.

80. Bujak M, Frangogiannis NG. The role of TGF-beta signaling in myocardial infarction and cardiac remodeling. Cardiovasc Res 2007 May 1; 74(2): 184-95.

81. Huynh ML, Fadok VA, Henson PM. Phosphatidylserine-dependent ingestion of apoptotic cells promotes TGF-beta1 secretion and the resolution of inflammation. J Clin Invest 2002 Jan; 109(1): 41-50.

82. Assoian RK, Komoriya A, Meyers CA, Miller DM, Sporn MB. Transforming growth factor-beta in human platelets. Identification of a major storage site, purification, and characterization. J Biol Chem 1983 Jun 10; 258(11): 7155-60.

83. Verrecchia F, Mauviel A. Transforming growth factor-beta and fibrosis. World J Gastroenterol 2007 Jun 14; 13(22): 3056-62.

84. Verrecchia F, Mauviel A, Farge D. Transforming growth factor-beta signaling through the Smad proteins: role in systemic sclerosis. Autoimmun Rev 2006 Oct; 5(8): 563-9.

85. Verrecchia F, Mauviel A, Farge D. Transforming growth factor-beta signaling through the Smad proteins: role in systemic sclerosis. Autoimmun Rev 2006 Oct; 5(8): 563-9.

86. Rahimi RA, Leof EB. TGF-beta signaling: a tale of two responses. J Cell Biochem 2007 Oct 15; 102(3): 593-608.

87. Annes JP, Munger JS, Rifkin DB. Making sense of latent TGFbeta activation 1. J Cell Sci 2003 Jan 15; 116(Pt 2): 217-24.

88. Ignotz RA, Massague J. Transforming growth factor-beta stimulates the expression of fibronectin and collagen and their incorporation into the extracellular matrix. J Biol Chem 1986 Mar 25; 261(9): 4337-45.

89. Rifkin DB, Mazzieri R, Munger JS, Noguera I, Sung J. Proteolytic control of growth factor availability. APMIS 1999 Jan; 107(1): 80-5.

90. Frangogiannis NG, Ren G, Dewald O, Zymek P, Haudek S, Koerting A, et al. Critical role of endogenous thrombospondin-1 in preventing expansion of healing myocardial infarcts. Circulation 2005 Jun 7; 111(22): 2935-42.

91. Barcellos-Hoff MH, Derynck R, Tsang ML, Weatherbee JA. Transforming growth factor-beta activation in irradiated murine mammary gland. J Clin Invest 1994 Feb; 93(2): 892-9.

92. Lyons RM, Keski-Oja J, Moses HL. Proteolytic activation of latent transforming growth factor-beta from fibroblast-conditioned medium. J Cell Biol 1988 May; 106(5): 1659-65.

93. Birdsall HH, Green DM, Trial J, Youker KA, Burns AR, MacKay CR, et al. Complement C5a, TGF-beta 1, and MCP-1, in sequence, induce migration of monocytes into ischemic canine myocardium within the first one to five hours after reperfusion. Circulation 1997 Feb 4; 95(3): 684-92.

94. Dean RG, Balding LC, Candido R, Burns WC, Cao Z, Twigg SM, et al. Connective tissue growth factor and cardiac fibrosis after myocardial infarction. J Histochem Cytochem 2005 Oct; 53(10): 1245-56.

95. Hao J, Ju H, Zhao S, Junaid A, Scammell-LaFleur T., Dixon IM. Elevation of expression of Smads 2, 3, and 4, decorin and TGF-beta in the chronic phase of myocardial infarct scar healing. J Mol Cell Cardiol 1999 Mar; 31(3): 667-78.

96. Wang B, Hao J, Jones SC, Yee MS, Roth JC, Dixon IM. Decreased Smad 7 expression contributes to cardiac fibrosis in the infarcted rat heart. Am J Physiol Heart Circ Physiol 2002 May; 282(5): H1685-H1696.

97. Bujak M, Frangogiannis NG. The role of TGF-beta signaling in myocardial infarction and cardiac remodeling. Cardiovasc Res 2007 May 1; 74(2): 184-95.

98. Smith WB, Noack L, Khew-Goodall Y, Isenmann S, Vadas MA, Gamble JR. Transforming growth factor-beta 1 inhibits the production of IL-8 and the transmigration of neutrophils through activated endothelium. J Immunol 1996 Jul 1; 157(1): 360-8.

99. Werner F, Jain MK, Feinberg MW, Sibinga NE, Pellacani A, Wiesel P, et al. Transforming growth factor-beta 1 inhibition of macrophage activation is mediated via Smad3. J Biol Chem 2000 Nov 24; 275(47): 36653-8.

100. Birdsall HH, Green DM, Trial J, Youker KA, Burns AR, MacKay CR, et al. Complement C5a, TGF-beta 1, and MCP-1, in sequence, induce migration of monocytes into ischemic canine myocardium within the first one to five hours after reperfusion. Circulation 1997 Feb 4; 95(3): 684-92.

101. Feinberg MW, Jain MK, Werner F, Sibinga NE, Wiesel P, Wang H, et al. Transforming growth factor-beta 1 inhibits cytokine-mediated induction of human metalloelastase in macrophages. J Biol Chem 2000 Aug 18; 275(33): 25766-73.

102. Werner F, Jain MK, Feinberg MW, Sibinga NE, Pellacani A, Wiesel P, et al. Transforming growth factor-beta 1 inhibition of macrophage activation is mediated via Smad3. J Biol Chem 2000 Nov 24; 275(47): 36653-8.

103. Kulkarni AB, Huh CG, Becker D, Geiser A, Lyght M, Flanders KC, et al. Transforming growth factor beta 1 null mutation in mice causes excessive inflammatory response and early death. Proc Natl Acad Sci U S A 1993 Jan 15; 90(2): 770-4.

104. Lijnen PJ, Petrov VV, Fagard RH. Induction of cardiac fibrosis by transforming growth factor-beta(1). Mol Genet Metab 2000 Sep; 71(1-2): 418-35.

105. Schiller M, Javelaud D, Mauviel A. TGF-beta-induced SMAD signaling and gene regulation: consequences for extracellular matrix remodeling and wound healing 1. J Dermatol Sci 2004 Aug; 35(2): 83-92.

106. Desmouliere A, Geinoz A, Gabbiani F, Gabbiani G. Transforming growth factor-beta 1 induces alpha-smooth muscle actin expression in granulation tissue myofibroblasts and in quiescent and growing cultured fibroblasts. J Cell Biol 1993; 122(1): 103-11.

107. Eghbali M, Tomek R, Sukhatme VP, Woods C, Bhambi B. Differential effects of transforming growth factor-beta 1 and phorbol myristate acetate on cardiac

fibroblasts. Regulation of fibrillar collagen mRNAs and expression of early transcription factors. Circ Res 1991; 69(2): 483-90.

108. Bujak M, Frangogiannis NG. The role of TGF-beta signaling in myocardial infarction and cardiac remodeling. Cardiovasc Res 2007 May 1; 74(2): 184-95.

109. Schiller M, Javelaud D, Mauviel A. TGF-beta-induced SMAD signaling and gene regulation: consequences for extracellular matrix remodeling and wound healing 1. J Dermatol Sci 2004 Aug; 35(2): 83-92.

110. Goumans MJ, Valdimarsdottir G, Itoh S, Rosendahl A, Sideras P, ten DP. Balancing the activation state of the endothelium via two distinct TGF-beta type I receptors. EMBO J 2002 Apr 2; 21(7): 1743-53.

111. Verrecchia F, Mauviel A. Transforming growth factor-beta and fibrosis. World J Gastroenterol 2007 Jun 14; 13(22): 3056-62.

112. Verrecchia F, Mauviel A, Farge D. Transforming growth factor-beta signaling through the Smad proteins: role in systemic sclerosis. Autoimmun Rev 2006 Oct; 5(8): 563-9.

113. Itoh S, Itoh F, Goumans MJ, ten Dijke P. Signaling of transforming growth factor-beta family members through Smad proteins. Eur J Biochem 2000; 267(24): 6954-67.

114. Raftery LA, Twombly V, Wharton K, Gelbart WM. Genetic screens to identify elements of the decapentaplegic signaling pathway in Drosophila. Genetics 1995 Jan; 139(1): 241-54.

115. Sekelsky JJ, Newfeld SJ, Raftery LA, Chartoff EH, Gelbart WM. Genetic characterization and cloning of mothers against dpp, a gene required for decapentaplegic function in Drosophila melanogaster. Genetics 1995; 139(3): 1347-58.

116. Savage C, Das P, Finelli AL, Townsend SR, Sun CY, Baird SE, et al. Caenorhabditis elegans genes sma-2, sma-3, and sma-4 define a conserved family of transforming growth factor beta pathway components. Proc Natl Acad Sci U S A 1996 Jan 23; 93(2): 790-4.

117. Hahn SA, Schutte M, Hoque AT, Moskaluk CA, da Costa LT, Rozenblum E, et al. DPC4, a candidate tumor suppressor gene at human chromosome 18q21.1. Science 1996 Jan 19; 271(5247): 350-3.

118. Derynck R, Gelbart WM, Harland RM, Heldin CH, Kern SE, Massague J, et al. Nomenclature: vertebrate mediators of TGFbeta family signals. Cell 1996; 87(2): 173.

119. Wrana JL, Attisano L. The Smad pathway. Cytokine Growth Factor Rev 2000; 11(1-2): 5-13.

120. Heldin CH, Miyazono K, ten Dijke P. TGF-beta signalling from cell membrane to nucleus through SMAD proteins. Nature 1997 Dec 4; 390(6659): 465-71.

121. Attisano L, Lee-Hoeflich ST. The Smads
18. Genome Biol 2001; 2(8): REVIEWS3010.

122. Shi Y. Structural insights on Smad function in TGFbeta signaling
3. Bioessays 2001 Mar; 23(3): 223-32.

123. Miyazawa K, Shinozaki M, Hara T, Furuya T, Miyazono K. Two major Smad pathways in TGF-beta superfamily signalling
17. Genes Cells 2002 Dec; 7(12): 1191-204.

124. Mehra A, Wrana JL. TGF-beta and the Smad signal transduction pathway
1. Biochem Cell Biol 2002; 80(5): 605-22.

125. Kretzschmar M, Liu F, Hata A, Doody J, Massague J. The TGF-beta family mediator Smad1 is phosphorylated directly and activated functionally by the BMP receptor kinase. Genes Dev 1997 Apr 15; 11(8): 984-95.

126. Abdollah S, Macias-Silva M, Tsukazaki T, Hayashi H, Attisano L, Wrana JL. TbetaRI phosphorylation of Smad2 on Ser465 and Ser467 is required for Smad2-Smad4 complex formation and signaling. J Biol Chem 1997; 272(44): 27678-85.

127. Shi Y. Crystal Structure of a Smad MH1 Domain Bound to DNA: Insights on DNA Binding in TGF-beta Signaling. Cell 1999; 94: 585-94.

128. Inman GJ. Linking Smads and transcriptional activation
1. Biochem J 2005 Feb 15; 386(Pt 1): e1-e3.

129. Qin BY, Lam SS, Correia JJ, Lin K. Smad3 allostery links TGF-beta receptor kinase activation to transcriptional control
3. Genes Dev 2002 Aug 1; 16(15): 1950-63.

130. Hahn SA, Schutte M, Hoque AT, Moskaluk CA, da Costa LT, Rozenblum E, et al. DPC4, a candidate tumor suppressor gene at human chromosome 18q21.1. [see comments]. Science 1996 Jan 19; 271(5247): 350-3.

131. Lagna G, Hata A, Hemmati-Brivanlou A, Massague J. Partnership between DPC4 and SMAD proteins in TGF-beta signalling pathways. Nature 1996 Oct 31; 383(6603): 832-6.

132. Zhang Y, Musci T, Derynck R. The tumor suppressor Smad4/DPC 4 as a central mediator of Smad function. Curr Biol 1997 Apr 1; 7(4): 270-6.

133. Wrana JL. The secret life of Smad4. Cell 2009 Jan 9; 136(1): 13-4.

134. Dupont S, Mamidi A, Cordenonsi M, Montagner M, Zacchigna L, Adorno M, et al. FAM/USP9x, a deubiquitinating enzyme essential for TGFbeta signaling, controls Smad4 monoubiquitination. Cell 2009 Jan 9; 136(1): 123-35.

135. Dupont S, Mamidi A, Cordenonsi M, Montagner M, Zacchigna L, Adorno M, et al. FAM/USP9x, a deubiquitinating enzyme essential for TGFbeta signaling, controls Smad4 monoubiquitination. Cell 2009 Jan 9; 136(1): 123-35.

136. Shi Y. Structural insights on Smad function in TGFbeta signaling
3. Bioessays 2001 Mar; 23(3): 223-32.

137. Zhang S, Fei T, Zhang L, Zhang R, Chen F, Ning Y, et al. Smad7 antagonizes transforming growth factor beta signaling in the nucleus by interfering with functional Smad-DNA complex formation
2. Mol Cell Biol 2007 Jun; 27(12): 4488-99.

138. Nakao A, Afrakhte M, Moren A, Nakayama T, Christian JL, Heuchel R, et al. Identification of Smad7, a TGFbeta-inducible antagonist of TGF-beta signalling. Nature 1997 Oct 9; 389(6651): 631-5.

139. Miyazono K. Positive and negative regulation of TGF-beta signaling. J Cell Sci 2000 Apr; 113 (Pt 7): 1101-9.

140. Nakao A, Afrakhte M, Moren A, Nakayama T, Christian JL, Heuchel R, et al. Identification of Smad7, a TGFbeta-inducible antagonist of TGF-beta signalling. Nature 1997 Oct 9; 389(6651): 631-5.

141. Hanyu A, Ishidou Y, Ebisawa T, Shimanuki T, Imamura T, Miyazono K. The N domain of Smad7 is essential for specific inhibition of transforming growth factor-beta signaling
2. J Cell Biol 2001 Dec 10; 155(6): 1017-27.

142. Murakami G, Watabe T, Takaoka K, Miyazono K, Imamura T. Cooperative inhibition of bone morphogenetic protein signaling by Smurf1 and inhibitory Smads. Mol Biol Cell 2003 Jul; 14(7): 2809-17.

143. Shi W, Sun C, He B, Xiong W, Shi X, Yao D, et al. GADD34-PP1c recruited by Smad7 dephosphorylates TGFbeta type I receptor
1. J Cell Biol 2004 Jan 19; 164(2): 291-300.

144. Ebisawa T, Fukuchi M, Murakami G, Chiba T, Tanaka K, Imamura T, et al. Smurf1 interacts with transforming growth factor-beta type I receptor through Smad7 and induces receptor degradation. J Biol Chem 2001 Apr; %20;276(16): 12477-80.

145. Kavsak P, Rasmussen RK, Causing CG, Bonni S, Zhu H, Thomsen GH, et al. Smad7 binds to Smurf2 to form an E3 ubiquitin ligase that targets the TGF beta receptor for degradation. Mol Cell 2000 Dec; 6(6): 1365-75.

146. Hata A, Lagna G, Massague J, Hemmati-Brivanlou A. Smad6 inhibits BMP/Smad1 signaling by specifically competing with the Smad4 tumor suppressor. Genes Dev 1998 Jan 15; 12(2): 186-97.

147. Murakami G, Watabe T, Takaoka K, Miyazono K, Imamura T. Cooperative inhibition of bone morphogenetic protein signaling by Smurf1 and inhibitory Smads. Mol Biol Cell 2003 Jul; 14(7): 2809-17.

148. Zhang S, Fei T, Zhang L, Zhang R, Chen F, Ning Y, et al. Smad7 antagonizes transforming growth factor beta signaling in the nucleus by interfering with functional Smad-DNA complex formation
2. Mol Cell Biol 2007 Jun; 27(12): 4488-99.

149. Massague J, Wotton D. Transcriptional control by the TGF-beta/Smad signaling system
5. EMBO J 2000 Apr 17; 19(8): 1745-54.

150. Bai S, Cao X. A nuclear antagonistic mechanism of inhibitory Smads in transforming growth factor-beta signaling. J Biol Chem 2002 Feb 8; 277(6): 4176-82.

151. Bai S, Shi X, Yang X, Cao X. Smad6 as a transcriptional corepressor
1. J Biol Chem 2000 Mar 24; 275(12): 8267-70.

152. Lin X, Liang YY, Sun B, Liang M, Shi Y, Brunicardi FC, et al. Smad6 recruits transcription corepressor CtBP to repress bone morphogenetic protein-induced transcription
1. Mol Cell Biol 2003 Dec; 23(24): 9081-93.

153. Li Y, Turck CM, Teumer JK, Stavnezer E. Unique sequence, ski, in Sloan-Kettering avian retroviruses with properties of a new cell-derived oncogene. J Virol 1986 Mar; 57(3): 1065-72.

154. Deheuninck J, Luo K. Ski and SnoN, potent negative regulators of TGF-beta signaling. Cell Res 2009 Jan; 19(1): 47-57.

155. Arndt S, Poser I, Moser M, Bosserhoff AK. Fussel-15, a novel Ski/Sno homolog protein, antagonizes BMP signaling. Mol Cell Neurosci 2007 Apr; 34(4): 603-11.

156. Arndt S, Poser I, Schubert T, Moser M, Bosserhoff AK. Cloning and functional characterization of a new Ski homolog, Fussel-18, specifically expressed in neuronal tissues. Lab Invest 2005 Nov; 85(11): 1330-41.

157. Kozmik Z, Pfeffer P, Kralova J, Paces J, Paces V, Kalousova A, et al. Molecular cloning and expression of the human and mouse homologues of the Drosophila dachshund gene. Dev Genes Evol 1999 Sep; 209(9): 537-45.

158. Wu K, Yang Y, Wang C, Davoli MA, D'Amico M, Li A, et al. DACH1 inhibits transforming growth factor-beta signaling through binding Smad4. J Biol Chem 2003 Dec 19; 278(51): 51673-84.

159. Wu JW, Krawitz AR, Chai J, Li W, Zhang F, Luo K, et al. Structural mechanism of Smad4 recognition by the nuclear oncoprotein Ski: insights on Ski-mediated repression of TGF-beta signaling. Cell 2002 Nov 1; 111(3): 357-67.

160. Heyman HC, Stavnezer E. A carboxyl-terminal region of the ski oncoprotein mediates homodimerization as well as heterodimerization with the related protein SnoN. J Biol Chem 1994 Oct 28; 269(43): 26996-7003.

161. Lyons GE, Micales BK, Herr MJ, Horrigan SK, Namciu S, Shardy D, et al. Protooncogene c-ski is expressed in both proliferating and postmitotic neuronal populations. Dev Dyn 1994 Dec; 201(4): 354-65.

162. Berk M, Desai SY, Heyman HC, Colmenares C. Mice lacking the ski proto-oncogene have defects in neurulation, craniofacial, patterning, and skeletal muscle development. Genes Dev 1997 Aug 15; 11(16): 2029-39.

163. Gajecka M, Mackay KL, Shaffer LG. Monosomy 1p36 deletion syndrome. Am J Med Genet C Semin Med Genet 2007 Nov 15; 145C(4): 346-56.

164. Colmenares C, Heilstedt HA, Shaffer LG, Schwartz S, Berk M, Murray JC, et al. Loss of the SKI proto-oncogene in individuals affected with 1p36 deletion syndrome is predicted by strain-dependent defects in Ski-/- mice. Nat Genet 2002 Jan; 30(1): 106-9.

165. Kobayashi N, Goto K, Horiguchi K, Nagata M, Kawata M, Miyazawa K, et al. c-Ski activates MyoD in the nucleus of myoblastic cells through suppression of histone deacetylases. Genes Cells 2007 Mar; 12(3): 375-85.

166. Atanasoski S, Notterpek L, Lee HY, Castagner F, Young P, Ehrengruber MU, et al. The protooncogene Ski controls Schwann cell proliferation and myelination. Neuron 2004 Aug 19; 43(4): 499-511.

167. Dahl R, Kieslinger M, Beug H, Hayman MJ. Transformation of hematopoietic cells by the Ski oncoprotein involves repression of retinoic acid receptor signaling. Proc Natl Acad Sci U S A 1998 Sep 15; 95(19): 11187-92.

168. Pearson-White S, Deacon D, Crittenden R, Brady G, Iscove N, Quesenberry PJ. The ski/sno protooncogene family in hematopoietic development. Blood 1995 Sep 15; 86(6): 2146-55.

169. Liu X, Zhang E, Li P, Liu J, Zhou P, Gu DY, et al. Expression and possible mechanism of c-ski, a novel tissue repair-related gene during normal and radiation-impaired wound healing. Wound Repair Regen 2006 Mar; 14(2): 162-71.

170. ias-Silva M, Li W, Leu JI, Crissey MA, Taub R. Up-regulated transcriptional repressors SnoN and Ski bind Smad proteins to antagonize transforming growth factor-beta signals during liver regeneration. J Biol Chem 2002 Aug 9; 277(32): 28483-90.

171. Fukuchi M, Nakajima M, Fukai Y, Miyazaki T, Masuda N, Sohda M, et al. Increased expression of c-Ski as a co-repressor in transforming growth factor-beta signaling correlates with progression of esophageal squamous cell carcinoma. Int J Cancer 2004 Mar 1; 108(6): 818-24.

172. Reed JA, Lin Q, Chen D, Mian IS, Medrano EE. SKI pathways inducing progression of human melanoma. Cancer Metastasis Rev 2005 Jun; 24(2): 265-72.

173. Buess M, Terracciano L, Reuter J, Ballabeni P, Boulay JL, Laffer U, et al. Amplification of SKI is a prognostic marker in early colorectal cancer. Neoplasia 2004 May; 6(3): 207-12.

174. Luo K, Stroschein SL, Wang W, Chen D, Martens E, Zhou S, et al. The Ski oncoprotein interacts with the Smad proteins to repress TGFbeta signaling. Genes Dev 1999 Sep 1; 13(17): 2196-206.

175. Akiyoshi S, Inoue H, Hanai J, Kusanagi K, Nemoto N, Miyazono K, et al. c-Ski acts as a transcriptional co-repressor in transforming growth factor-beta signaling through interaction with smads. J Biol Chem 1999 Dec 3; 274(49): 35269-77.

176. Sun Y, Liu X, Eaton EN, Lane WS, Lodish HF, Weinberg RA. Interaction of the Ski oncoprotein with Smad3 regulates TGF-beta signaling. Mol Cell 1999 Oct; 4(4): 499-509.

177. Xu W, Angelis K, Danielpour D, Haddad MM, Bischof O, Campisi J, et al. Ski acts as a co-repressor with Smad2 and Smad3 to regulate the response to type beta transforming growth factor. Proc Natl Acad Sci U S A 2000 May 23; 97(11): 5924-9.

178. Wu JW, Krawitz AR, Chai J, Li W, Zhang F, Luo K, et al. Structural mechanism of Smad4 recognition by the nuclear oncoprotein Ski: insights on Ski-mediated repression of TGF-beta signaling. Cell 2002 Nov 1; 111(3): 357-67.

179. Harada J, Kokura K, Kanei-Ishii C, Nomura T, Khan MM, Kim Y, et al. Requirement of the co-repressor homeodomain-interacting protein kinase 2 for ski-mediated inhibition of bone morphogenetic protein-induced transcriptional activation
1. J Biol Chem 2003 Oct 3; 278(40): 38998-9005.

180. Nomura T, Khan MM, Kaul SC, Dong HD, Wadhwa R, Colmenares C, et al. Ski is a component of the histone deacetylase complex required for transcriptional repression by Mad and thyroid hormone receptor. Genes Dev 1999 Feb 15; 13(4): 412-23.

181. Ayer DE, Lawrence QA, Eisenman RN. Mad-Max transcriptional repression is mediated by ternary complex formation with mammalian homologs of yeast repressor Sin3
1. Cell 1995 Mar 10; 80(5): 767-76.

182. Akiyoshi S, Inoue H, Hanai J, Kusanagi K, Nemoto N, Miyazono K, et al. c-Ski acts as a transcriptional co-repressor in transforming growth factor-beta signaling through interaction with smads. J Biol Chem 1999 Dec 3; 274(49): 35269-77.

183. Wu JW, Krawitz AR, Chai J, Li W, Zhang F, Luo K, et al. Structural mechanism of Smad4 recognition by the nuclear oncoprotein Ski: insights on Ski-mediated repression of TGF-beta signaling. Cell 2002 Nov 1; 111(3): 357-67.

184. Sakuma-Takagi M, Tohyama Y, Kasama-Yoshida H, Sakagami H, Kondo H, Kurihara T. Novel related cDNAs (C184L, C184M, and C184S) from developing mouse brain encoding two apparently unrelated proteins
3. Biochem Biophys Res Commun 1999 Oct 5; 263(3): 737-42.

185. Muro Y, Yamada T, Himeno M, Sugimoto K. cDNA cloning of a novel autoantigen targeted by a minor subset of anti-centromere antibodies
1. Clin Exp Immunol 1998 Feb; 111(2): 372-6.

186. Golovkina TV, Dzuris J, van den HB, Jaffe AB, Wright PC, Cofer SM, et al. A novel membrane protein is a mouse mammary tumor virus receptor
1. J Virol 1998 Apr; 72(4): 3066-71.

187. Kokura K, Kim H, Shinagawa T, Khan MM, Nomura T, Ishii S. The Ski-binding protein C184M negatively regulates tumor growth factor-beta signaling by sequestering the Smad proteins in the cytoplasm. J Biol Chem 2003 May 30; 278(22): 20133-9.

188. Kokura K, Kim H, Shinagawa T, Khan MM, Nomura T, Ishii S. The Ski-binding protein C184M negatively regulates tumor growth factor-beta signaling by sequestering the Smad proteins in the cytoplasm. J Biol Chem 2003 May 30; 278(22): 20133-9.

189. Kokura K, Kim H, Shinagawa T, Khan MM, Nomura T, Ishii S. The Ski-binding protein C184M negatively regulates tumor growth factor-beta signaling by sequestering the Smad proteins in the cytoplasm. J Biol Chem 2003 May 30; 278(22): 20133-9.

190. Brilla CG, Zhou G, Matsubara L, Weber KT. Collagen metabolism in cultured adult rat cardiac fibroblasts: response to angiotensin II and aldosterone. J Mol Cell Cardiol 1994; 26(7): 809-20.

191. Ju H, Hao J, Zhao S, Dixon IMC. Antiproliferative and antifibrotic effects of mimosine on adult cardiac fibroblasts. Biochim Biophys Acta 1998 Nov 19; 1448(1): 51-60.

192. Smith PK, Krohn RI, Hermanson GT, Mallia AK, Gartner FH, Provenzano MD, et al. Measurement of protein using bicinchoninic acid. Anal Biochem 1985; 150(1): 76-85.

193. Wu Z, Nagano I, Boonmars T, Takahashi Y. Involvement of the c-Ski oncoprotein in cell cycle arrest and transformation during nurse cell formation after Trichinella spiralis infection
3. Int J Parasitol 2006 Sep; 36(10-11): 1159-66.

194. Sakuma-Takagi M, Tohyama Y, Kasama-Yoshida H, Sakagami H, Kondo H, Kurihara T. Novel related cDNAs (C184L, C184M, and C184S) from developing mouse brain encoding two apparently unrelated proteins
3. Biochem Biophys Res Commun 1999 Oct 5; 263(3): 737-42.

195. Roberts AB, Heine UI, Flanders KC, Sporn MB. Transforming growth factor-beta. Major role in regulation of extracellular matrix. Ann N Y Acad Sci 1990; 580:225-32: 225-32.

196. Massague J. The transforming growth factor-beta family. Annu Rev Cell Biol 1990; 6: 597-641.

197. Arany PR, Flanders KC, Kobayashi T, Kuo CK, Stuelten C, Desai KV, et al. Smad3 deficiency alters key structural elements of the extracellular matrix and mechanotransduction of wound closure. Proc Natl Acad Sci U S A 2006 Jun 13; 103(24): 9250-5.

198. Sakuma-Takagi M, Tohyama Y, Kasama-Yoshida H, Sakagami H, Kondo H, Kurihara T. Novel related cDNAs (C184L, C184M, and C184S) from developing mouse brain encoding two apparently unrelated proteins
3. Biochem Biophys Res Commun 1999 Oct 5; 263(3): 737-42.

199. Kokura K, Kim H, Shinagawa T, Khan MM, Nomura T, Ishii S. The Ski-binding protein C184M negatively regulates tumor growth factor-beta signaling by sequestering the Smad proteins in the cytoplasm. J Biol Chem 2003 May 30; 278(22): 20133-9.

200. Kokura K, Kim H, Shinagawa T, Khan MM, Nomura T, Ishii S. The Ski-binding protein C184M negatively regulates tumor growth factor-beta signaling by sequestering the Smad proteins in the cytoplasm. J Biol Chem 2003 May 30; 278(22): 20133-9.

201. Kokura K, Kim H, Shinagawa T, Khan MM, Nomura T, Ishii S. The Ski-binding protein C184M negatively regulates tumor growth factor-beta signaling by sequestering the Smad proteins in the cytoplasm. J Biol Chem 2003 May 30; 278(22): 20133-9.

202. Deheuninck J, Luo K. Ski and SnoN, potent negative regulators of TGF-beta signaling. Cell Res 2009 Jan; 19(1): 47-57.

203. Hao J, Ju H, Zhao S, Junaid A, Scammell-LaFleur T., Dixon IM. Elevation of expression of Smads 2, 3, and 4, decorin and TGF-beta in the chronic phase of myocardial infarct scar healing. J Mol Cell Cardiol 1999 Mar; 31(3): 667-78.

204. Kokura K, Kim H, Shinagawa T, Khan MM, Nomura T, Ishii S. The Ski-binding protein C184M negatively regulates tumor growth factor-beta signaling by sequestering the Smad proteins in the cytoplasm. J Biol Chem 2003 May 30; 278(22): 20133-9.

205. Bujak M, Frangogiannis NG. The role of TGF-beta signaling in myocardial infarction and cardiac remodeling. Cardiovasc Res 2007 May 1; 74(2): 184-95.

206. Kuwahara F, Kai H, Tokuda K, Kai M, Takeshita A, Egashira K, et al. Transforming growth factor-beta function blocking prevents myocardial fibrosis and diastolic dysfunction in pressure-overloaded rats. Circulation 2002 Jul 2; 106(1): 130-5.

207. Bujak M, Frangogiannis NG. The role of TGF-beta signaling in myocardial infarction and cardiac remodeling. Cardiovasc Res 2007 May 1; 74(2): 184-95.

208. Lijnen PJ, Petrov VV, Fagard RH. Induction of cardiac fibrosis by transforming growth factor-beta(1). Mol Genet Metab 2000 Sep; 71(1-2): 418-35.

209. Kossmehl P, Schonberger J, Shakibaei M, Faramarzi S, Kurth E, Habighorst B, et al. Increase of fibronectin and osteopontin in porcine hearts following ischemia and reperfusion. J Mol Med 2005 Aug; 83(8): 626-37.

210. Petrov VV, Fagard RH, Lijnen PJ. Stimulation of collagen production by transforming growth factor-beta1 during differentiation of cardiac fibroblasts to myofibroblasts. Hypertension 2002; 39(2): 258-63.

211. Kossmehl P, Schonberger J, Shakibaei M, Faramarzi S, Kurth E, Habighorst B, et al. Increase of fibronectin and osteopontin in porcine hearts following ischemia and reperfusion. J Mol Med 2005 Aug; 83(8): 626-37.

212. Kokura K, Kim H, Shinagawa T, Khan MM, Nomura T, Ishii S. The Ski-binding protein C184M negatively regulates tumor growth factor-beta signaling by sequestering the Smad proteins in the cytoplasm. J Biol Chem 2003 May 30; 278(22): 20133-9.

213. Sun Y, Liu X, Eaton EN, Lane WS, Lodish HF, Weinberg RA. Interaction of the Ski oncoprotein with Smad3 regulates TGF-beta signaling. Mol Cell 1999 Oct; 4(4): 499-509.

214. Xu W, Angelis K, Danielpour D, Haddad MM, Bischof O, Campisi J, et al. Ski acts as a co-repressor with Smad2 and Smad3 to regulate the response to type beta transforming growth factor. Proc Natl Acad Sci U S A 2000 May 23; 97(11): 5924-9.

215. Wang W, Mariani FV, Harland RM, Luo K. Ski represses bone morphogenic protein signaling in Xenopus and mammalian cells. Proc Natl Acad Sci U S A 2000 Dec 19; 97(26): 14394-9.

216. Reed JA, Bales E, Xu W, Okan NA, Bandyopadhyay D, Medrano EE. Cytoplasmic localization of the oncogenic protein Ski in human cutaneous melanomas in vivo: functional implications for transforming growth factor beta signaling. Cancer Res 2001 Nov 15; 61(22): 8074-8.

217. Grimm OH, Gurdon JB. Nuclear exclusion of Smad2 is a mechanism leading to loss of competence
1. Nat Cell Biol 2002 Jul; 4(7): 519-22.

218. Kokura K, Kim H, Shinagawa T, Khan MM, Nomura T, Ishii S. The Ski-binding protein C184M negatively regulates tumor growth factor-beta signaling by sequestering the Smad proteins in the cytoplasm. J Biol Chem 2003 May 30; 278(22): 20133-9.

219. Namciu S, Lyons GE, Micales BK, Heyman HC, Colmenares C, Stavnezer E. Enhanced expression of mouse c-ski accompanies terminal skeletal muscle differentiation in vivo and in vitro. Dev Dyn 1995 Nov; 204(3): 291-300.

220. Berk M, Desai SY, Heyman HC, Colmenares C. Mice lacking the ski proto-oncogene have defects in neurulation, craniofacial, patterning, and skeletal muscle development. Genes Dev 1997 Aug 15; 11(16): 2029-39.

221. Frangogiannis NG, Michael LH, Entman ML. Myofibroblasts in reperfused myocardial infarcts express the embryonic form of smooth muscle myosin heavy chain (SMemb). Cardiovasc Res 2000 Oct; 48(1): 89-100.

222. Kokura K, Kim H, Shinagawa T, Khan MM, Nomura T, Ishii S. The Ski-binding protein C184M negatively regulates tumor growth factor-beta signaling by sequestering the Smad proteins in the cytoplasm. J Biol Chem 2003 May 30; 278(22): 20133-9.